Transport in Porous Media (2006) 63: 13–56
DOI 10.1007/s11242-005-1291-7

A Two-Scale Model for Coupled Electro-Chemo-Mechanical Phenomena and Onsager's Reciprocity Relations in Expansive Clays: II Computational Validation

CHRISTIAN MOYNE[1] and MÁRCIO A. MURAD[2]
[1]*LEMTA–CNRS–INPL–UHP (UMR 7563) 2, avenue de la Forêt de Haye, 54504 Vandoeuvre lès Nancy Cedex, France*
[2]*Laboratório Nacional de Computação Científica LNCC/MCT Av Getúlio Vargas 333, 25651–070 Petrópolis, RJ, Brazil*

(Received: 26 October 2004; accepted: 22 January 2005)

Abstract. In Part I Moyne and Murad [*Transport in Porous Media* **62**, (2006), 333–380] a two-scale model of coupled electro-chemo-mechanical phenomena in swelling porous media was derived by a formal asymptotic homogenization analysis. The microscopic portrait of the model consists of a two-phase system composed of an electrolyte solution and colloidal clay particles. The movement of the liquid at the microscale is ruled by the modified Stokes problem; the advection, diffusion and electro-migration of monovalent ions Na^+ and Cl^- are governed by the Nernst–Planck equations and the local electric potential distribution is dictated by the Poisson problem. The microscopic governing equations in the fluid domain are coupled with the elasticity problem for the clay particles through boundary conditions on the solid–fluid interface. The up-scaling procedure led to a macroscopic model based on Onsager's reciprocity relations coupled with a modified form of Terzaghi's effective stress principle including an additional swelling stress component. A notable consequence of the two-scale framework are the new closure problems derived for the macroscopic electro-chemo-mechanical parameters. Such local representation bridge the gap between the macroscopic Thermodynamics of Irreversible Processes and microscopic Electro-Hydrodynamics by establishing a direct correlation between the magnitude of the effective properties and the electrical double layer potential, whose local distribution is governed by a microscale Poisson–Boltzmann equation. The purpose of this paper is to validate computationally the two-scale model and to introduce new concepts inherent to the problem considering a particular form of microstructure wherein the clay fabric is composed of parallel particles of face-to-face contact. By discretizing the local Poisson–Boltzmann equation and solving numerically the closure problems, the constitutive behavior of the diffusion coefficients of cations and anions, chemico-osmotic and electro-osmotic conductivities in Darcy's law, Onsager's parameters, swelling pressure, electrochemical compressibility, surface tension, primary/secondary electroviscous effects and the reflection coefficient are computed for a range particle distances and sat concentrations.

Key words: swelling clay, stratified microstructure, Poisson–Boltzmann, Onsager's parameters, electro-osmotic permeability, chemico-osmotic permeability swelling pressure, reflection coefficient, electroviscous effect surface tension, numerical elliptic integrals.

1. Introduction

In a companion paper (Moyne and Murad, 2006), the authors proposed a two-scale model to describe coupled electro-chemo-mechanical phenomena in expansive porous media. The model was derived within the framework of homogenization (Bensoussan *et al.*, 1978; Sanchez-Palencia, 1980; Auriault, 1991) applied to up-scale the microscopic governing equations which consist of the elasticity problem for the clay particles coupled through boundary conditions with the electro-hydrodynamics, Nernst–Planck relations and Poisson problem governing the fluid movement, transport of mobile charges and electric potential distribution in the electrolyte solution occupying the micro-pores. (Landau and Lifshitz, 1960; Eringen and Maugin (1989); Samson and Marchand, 1999).

By defining the perturbation parameter ϵ of the homogenization procedure as the ratio between the microscopic scale (of the order of the Debye's length) and the macroscopic characteristic scale (of the order of magnitude of the size of the clay aggregates), unlike earlier work developed by the authors (Moyne and Murad, 2002, 2003); the up-scaling procedure adopted in Moyne and Murad (2006) considered the macroscopic Péclet number of $\mathcal{O}(1)$. This higher-order estimate combined with the asymptotic expansion technique led to a more realistic macroscopic picture of the swelling medium wherein new small-scale features, such as the influence of local distortion and relaxation of the charge cloud upon the magnitude of ion dispersivities and fluid conductivities in Darcy's law have been captured by the homogenized model.

In the macroscopic governing equations the Darcy's seepage velocity, total flux of species and electric current appear linearly related to the gradients of pressure, concentration and macroscopic electric potential through Onsager's reciprocity relations. This system is coupled with mass conservations for the fluid and species and with a modified form of Terzaghi's decomposition including an additional swelling stress tensor component (Sridharan and Rao, 1973; Hueckel, 1992; Murad and Cushman, 2000). In addition, local closure problems posed on a periodic unit cell are obtained for the electro-chemo-mechanical parameters. Such closure relations provide further insight in the physics underlying each effective coefficient by establishing a direct correlation with the microscopic electric double layer potential satisfying a local version of the Poisson–Boltzmann problem. In addition, other relevant information in the closure relations appears

incorporated in the additional nonequilibrium characteristic functions associated with tortuosity and distortion of the charge cloud induced by the advection. Finally, the closure problems are also capable of establishing the microscopic conditions for the symmetry of Onsager's matrix (see Moyne and Murad, 2006 for details).

The purpose of this article is twofold: to validate computationally the two-scale model proposed in Moyne and Murad (2006) and to introduce other relevant concepts inherent to the problem for a particular clay morphology. To this end we discretize the closure problems considering a stratified microstructure where the compacted swelling medium is composed of parallel particles of face-to-face contact. In this arrangement the local Poisson–Boltzmann equation reduces to a one-dimensional non-linear problem in the direction normal to the clay surface which is solved using a suitable change of variables in conjunction with an iterative numerical integration of elliptic integrals (Derjaguin *et al.*, 1987). The solution leads to the numerical profile of the microscale electric potential parametrized by salinity and distance between two parallel particles. We then make use of this discrete electrical double layer potential distribution to compute the chemico-osmotic and electro-osmotic velocity profiles. The transversal averaging of these local distributions (normally to the solid wall) yields the constitutive dependence of the diagonal components of the chemico-osmotic and electro-osmotic permeabilities (in the axial direction parallel to the particle surface) on salinity and particle distance. In addition, by solving numerically the other closure problems we compute the constitutive behavior of the macroscopic diffusion coefficients of cations and anions, swelling pressure, electro-chemical compressibility and Onsager's coefficients, also parametrized by salinity and particle distance. The two-scale computations presented herein aim at providing a first attempt at understanding the complex features underlying the constitutive nature of the electro-chemo-mechanical coefficients in swelling systems.

We also proceed beyond the two-scale computations for the effective coefficients defined in Moyne and Murad (2006) by further introducing other macroscopic concepts restricted to microgeometries composed of parallel particles. By noting that at equilibrium the stress state in the fluid is anisotropic in addition to the excess in pressure normal to the particle surface, quantified by the disjoining pressure (Derjaguin and Churaev, 1978), we also introduce the interfacial and surface tensions of the electrolyte solution by averaging the excess of the component of the fluid stress tensor tangential to the particles relative to the normal and bulk phase pressures. We show that these components arise from the sum of the Donnan-osmotic pressure and Maxwell components of the fluid stress tensor. By establishing a microscopic representation for these quantities, we compute their dependence on salinity and particle distance and show that their magnitude is

much higher than the swelling pressure, though they have no effect on swelling since their action is to compress the liquid in the direction parallel to the clay surface.

The consequences of the two-scale model are also exploited under some particular macroscopic constraints. More precisely we analyze the performance of the formulation under the open-circuit condition which is characterized by the absence of a macroscopic electric current (Gu *et al.*, 1998). Under this constraint the macroscale electric potential reduces to the so-called streaming potential, whose spatial variability opposes the pressure-driven flow, acting to slow down the counter-ions of the diffuse double layer and to reduce the mobility of the water molecules to fulfill the condition of zero net current (see Yang and Li, 1998 for details). By making use of this constraint we eliminate the streaming potential gradient in Onsager's relation for the electric current and rewrite the other reciprocity relations in terms of pressure and concentration gradients. In this scenario we introduce the membrane potential in the sense of Gu *et al.* (1998) as the total driving force for fluid flow and the so-called primary/secondary electro-viscous effects as a measure of the increase of the apparent viscosity of the fluid owing to the electro osmotic flow induced by the streaming potential gradient in the opposite direction of the hydraulic gradient. By establishing a closure problem for this quantity its constitutive dependence on salinity and particle distance is computed. Furthermore, still under the open-circuit assumption, we consider the movement of the water as a solvent and introduce the notion of reflection coefficient. Classically such concept was firstly introduced to quantify the nonideal behavior of semi-permeable membranes to the passage of nonionic species. Owing to the larger size of the solute molecules, the ideal behavior of a semi-permeable membrane, to which an unitary reflection coefficient is associated, occurs when the membrane is totally impervious to the passage of solutes and the movement of the solution is that of the solvent driven by its chemical-potential gradient. The partial mobility of solutes tends to deviate the membrane from its ideal behavior reducing the magnitude of the reflection coefficient to values less than unity. As the movement of charged species is constrained owing to their electro-chemico interactions with the clay, a proper characterization of reflection coefficient in this scenario becomes a relevant issue (see, e.g., Kemper and Schaik, 1966). Indeed, the reader shall be aware that this parameter has a totally different physical meaning compared to the case of larger size nonionic species. Likewise the other parameters, by establishing a proper definition for this quantity within the open-circuit assumption we derive its microscopic representation and discretize the local closure problem to obtain numerically the constitutive dependence of this parameter on salinity and particle distance.

Although the two-scale computations performed herein are restricted to a particular form of microstructure they provide guidance for a further development of an accurate constitutive theory of swelling porous media with random microgeometries capable of capturing the correct physics and particular assumptions underlying the characterization of each electro-chemo-mechanical parameter.

A brief outline of the paper is as follows: In Section 2 we review the main aspects of the two-scale model. In Section 3 we rephrase the closure problems for stratified microstructures and further manipulate them. In addition, we make use of the open circuit assumption and formally introduce the electroviscous effect and reflection coefficient. In Section 4 we present the discretization technique of the Poisson–Boltzmann equation and compute the solution of the closure problems. Finally, numerical simulations depict the behavior of the effective coefficients as a function of salinity and particle distance.

2. Review of the Homogenized Results

Let Ω be a macroscopic domain occupied by a mixture of uniformly negatively charged clay particles saturated by a dielectric aqueous solution with binary monovalent completely dissociated electrolytes Na^+ and Cl^-. The aqueous phase is considered a dilute solution with the ions treated as point charges at infinite dilution such that steric and hydration effects are neglected. For each macroscopic location $x \in \Omega$, the microscopic behavior of the swelling medium is represented by a continuous distribution of local problems posed in a periodic cell $Y = Y_f \cap Y_s$ with prescribed geometry and boundary ∂Y_{fs} (here the subscripts f and s denote the sub-domains occupied by the fluid and solid). The solution of the closure problems in each cell represents the influence of the microstructure near each macroscopic location x.

2.1. SUMMARY OF THE TWO-SCALE FORMULATION

We consider a thermodynamic process of the swelling medium characterized by a macroscopic time scale t. The system is assumed to exhibit the scale-separation property so that we can assign a perturbation parameter $\epsilon = \ell/L \ll 1$ with ℓ and L denoting the microscopic and macroscopic scales. The former scale is assumed of the order of the Debye's length (Van Olphen, 1977; Hunter, 1981) whereas the latter of the same magnitude of the clay aggregates.

Following the notation of Moyne and Murad (2006) $\{e^j\}$, $(j = 1, 2, 3)$ denotes an orthonormal basis and $\boldsymbol{I}$ designates the identity tensor represented

in components as $\delta^{ij}\boldsymbol{e}^i \otimes \boldsymbol{e}^j$ (sum on i, j with δ^{ij} and $\otimes$ denoting the Kronecker delta symbol and the tensorial product between vectors. We also adopt the notation $\boldsymbol{II}$ for the fourth-order unit tensor with components $\delta^{ij}\delta^{kl}$ and $\boldsymbol{A} : \boldsymbol{B}$ to represent the classical inner product between tensors $(A^{ij}B^{ij})$. The pair $\{\nabla_x, \nabla_y\}$ denotes the spatial gradient with respect to the macroscopic and microscopic coordinates $\boldsymbol{x}$ and $\boldsymbol{y}$ respectively. To simplify the notation and avoid the proliferation of symbols, we omit the superscript "0" adopted in Moyne and Murad (2006) to represent the $\mathcal{O}(\epsilon^0)$ component of the asymptotic expansion of each unknown.

Neglecting, gravity, convective, inertial effects and considering that the solid matrix undergoes small deformations with respect to an initial contact stress free configuration, the two-scale model derived in Moyne and Murad (2004, submitted) consists in finding the following variables (functions of $(\boldsymbol{x}, t)$): the macroscopic overall stress tensor $\boldsymbol{\sigma}_T$; the displacement of the solid particles $\mathbf{u}$; the macroscopic deformation of the solid matrix $\boldsymbol{\mathcal{E}}_x(\mathbf{u})$; the Biot's (1941) elastic contact stress $\boldsymbol{\sigma}_e$; the reference bulk pressure p_b of the fluid; the Darcy's velocity $\mathbf{v}_D$; the bulk concentration c_b; the macroscopic dimensionless electric potential $\bar{\psi}_b$; the fluxes of cations/anions $\boldsymbol{J}_\pm$ and the porosity n_f satisfying

Overall Momentum Balance

$$\nabla_x \cdot \boldsymbol{\sigma}_T = 0.$$

Modified Terzaghi's Decomposition

$$\boldsymbol{\sigma}_T = -\boldsymbol{\alpha} p_b + \boldsymbol{\sigma}_e - \Pi.$$

Linear Elastic Constitutive Law for the Contact Stresses

$$\boldsymbol{\sigma}_e - \boldsymbol{C}_s \boldsymbol{\mathcal{E}}_x(\mathbf{u}).$$

Small Strain Assumption

$$\boldsymbol{\mathcal{E}}_x(\mathbf{u}) = \tfrac{1}{2}\left(\nabla_x \mathbf{u} + (\nabla_x \mathbf{u})^T\right).$$

Modified Darcy's Law

$$\mathbf{v}_D = -\boldsymbol{K}_P \nabla_x p_b - \boldsymbol{K}_C \nabla_x c_b - \boldsymbol{K}_E \nabla_x \bar{\psi}_b. \tag{2.1}$$

Overall Mass Balance

$$\nabla_x \cdot \mathbf{v}_D + \boldsymbol{\alpha} : \frac{\partial}{\partial t} \boldsymbol{\mathcal{E}}_x(\mathbf{u}) = \beta \frac{\partial p_b}{\partial t} + \frac{\partial \gamma_\pi}{\partial t}.$$

Mass Balance of the Charged Species

$$\frac{\partial}{\partial t}(n_f G_\pm c_b) + \nabla_x \cdot \boldsymbol{J}_\pm = 0. \tag{2.2}$$

Nernst–Planck Relations

$$\boldsymbol{J}_{\pm} = c_{\mathrm{b}} G_{\pm} \mathbf{v}_{\pm} - n_{\mathrm{f}} \left(\boldsymbol{D}^{\mathrm{c}}_{\pm} \nabla_x c_{\mathrm{b}} \pm \boldsymbol{D}^{\mathrm{e}}_{\pm} c_{\mathrm{b}} \nabla_x \bar{\psi}_{\mathrm{b}} + \boldsymbol{D}^{\mathrm{p}}_{\pm} \nabla_x p_{\mathrm{b}} \right). \tag{2.3}$$

Mass Balance of the Fluid Phase

$$\frac{\partial n_{\mathrm{f}}}{\partial t} + \nabla_x \cdot \mathbf{v}_{\mathrm{D}} + n_{\mathrm{f}} \nabla_x \cdot \frac{\partial \mathbf{u}}{\partial t} = 0 \quad \text{in } \Omega.$$

In the above set of effective coefficients the pair $\{\mathbf{C}_{\mathrm{s}}, \boldsymbol{\alpha}\}$ denotes the elastic modulus of the clay matrix and a tensorial generalization of the Biot–Willis parameter; $\{\boldsymbol{K}_{\mathrm{P}}, \boldsymbol{K}_{\mathrm{C}}, \boldsymbol{K}_{\mathrm{E}}\}$ are the hydraulic, chemico-osmotic and electro-osmotic conductivities in Darcy's law; β and $\gamma_{\bar{\pi}}$ are the mechanical and electro-chemical compressibilities of the clay; $\boldsymbol{D}^{I}_{\pm}(\boldsymbol{I} = \mathrm{p}, \mathrm{c}, \mathrm{e})$ designate the diffusivities of the ions with respect to unitary gradients in bulk pressure, concentration and electric potential; $G_{\pm}$ are the cation/anion exchange capacities with the electrical double layer; $\mathbf{v}_{\pm}$ the averaged advection velocities of the ions and Π a macroscopic stress tensor which governs the electro-chemical interaction between the electrolyte solution and the macromolecules.

To depict the closure problems for the effective coefficients we begin by presenting the notation adopted herein. Denote $n_{\mathrm{s}} = 1 - n_{\mathrm{f}}$ the volume fraction of the solid phase, $\langle \cdot \rangle \equiv |Y|^{-1} \int_{Y_\alpha} \mathrm{d}Y$ the average operator over Y and $\langle \cdot \rangle^{\alpha} \equiv |Y_\alpha|^{-1} \int_{Y_\alpha} \mathrm{d}Y_\alpha (\alpha = \mathrm{f}, \mathrm{s})$ the intrinsic volume average operator over the α-portion of the unit cell Y so that $\langle \cdot \rangle = n_\alpha \langle \cdot \rangle^{\alpha}$. The set of microscopic properties $\{F, T, R, c_{\mathrm{s}}, \tilde{\varepsilon}_0, \tilde{\varepsilon}, \mathcal{D}_{\pm}, \mu_{\mathrm{f}}\}$, designates Faraday's constant, absolute temperature (assumed constant), universal ideal gas constant, fourth-order elastic modulus of the particles, permittivity of the free space, relative dielectric constant of the solvent, binary water-ions diffusion coefficients and fluid viscosity, respectively. We also introduce the Debye's length $\ell_D \equiv (\tilde{\varepsilon}\tilde{\varepsilon}_0 RT / 2F^2 c_{\mathrm{b}})^{1/2}$ which refers to as the characteristic length scale where the effects of the electrical double layer (e, d, l) become pronounced. For microscopically isotropic particles the components of the fourth-order elastic modulus of the solid admit the well-known representation $c^{ijkl} = \lambda_{\mathrm{s}} \delta^{ij} \delta^{kl} + \mu_{\mathrm{s}} \left(\delta^{ik} \delta^{jl} + \delta^{il} \delta^{jk} \right)$ with $\{\lambda_{\mathrm{s}}, \mu_{\mathrm{s}}\}$, denoting the pair of microscopic Lamé constants of the particles.

Our set of primary microscopic unknowns is $\left\{ \bar{\varphi}, \boldsymbol{E}, \pi, \boldsymbol{\tau}_M, \boldsymbol{\Pi}_{\mathrm{d}}, \mathbf{v}, \mathrm{p}, \boldsymbol{\sigma}_{\mathrm{f}}, \mathbf{u}_{\pi} \right\}$ which denote a dimensionless e.d.l. potential relative to $\bar{\psi}_b$ (denoted herein as an e.d.l. potential), electric field, osmotic pressure, Maxwell stress tensor, disjoining stress, local fluid velocity, thermodynamic pressure, stress tensor of the electrolyte solution and fluctuating displacement of the clay particles induced by electro-chemical effects. The relations between these microscopic variables are Moyne and Murad (2006)

$$
\begin{aligned}
&\boldsymbol{\Pi}_d = \pi \boldsymbol{I} - \boldsymbol{\tau_M}, \quad \pi = 2RTc_{\mathrm{b}}(\cosh\bar{\varphi} - 1),\\
&\boldsymbol{\tau}_M = \frac{\tilde{\varepsilon}\tilde{\varepsilon}_0}{2}(2\boldsymbol{E}\otimes\boldsymbol{E} - E^2\boldsymbol{I}),\\
&\mathbf{v} - \frac{\partial \mathbf{u}}{\partial t} = -\boldsymbol{\kappa}_{\mathrm{p}}\nabla_x p_{\mathrm{b}} - \boldsymbol{\kappa}_{\mathrm{c}}\nabla_x c_{\mathrm{b}} - \boldsymbol{\kappa}_{\mathrm{e}}\nabla_x \bar{\psi}_{\mathrm{b}},\\
&\boldsymbol{\sigma}_{\mathrm{f}} = -p\boldsymbol{I} + \boldsymbol{\tau}_M = -(p_{\mathrm{b}} + \pi)\boldsymbol{I} + \boldsymbol{\tau}_M = -p_{\mathrm{b}}\boldsymbol{I} - \boldsymbol{\Pi}_{\mathrm{d}},
\end{aligned}
\tag{2.4}
$$

where $\{\boldsymbol{\kappa}_{\mathrm{p}}, \boldsymbol{\kappa}_{\mathrm{c}}, \boldsymbol{\kappa}_{\mathrm{e}}\}$ is a set of characteristic velocity profiles induced by unitary hydraulic, chemico-osmotic and electro-osmotic gradients. Denoting $\mathcal{E}_y(\mathbf{u}) = 1/2(\nabla_y\mathbf{u} + (\nabla_y\mathbf{u})^T)$, the unknowns $\{\bar{\varphi}, \boldsymbol{E}, \mathbf{u}_\pi\}$ satisfy the Poisson–Boltzmann and elasticity problems with Neumann boundary conditions

$$
\begin{array}{l|l}
\Delta_{yy}\bar{\varphi} = (\ell_{\mathrm{D}}^2)^{-1}\sinh\bar{\varphi} & \\
\boldsymbol{E} = -RTF^{-1}\nabla_y\bar{\varphi} \quad \text{in } Y_{\mathrm{f}} & \nabla_y\cdot(\boldsymbol{c}_{\mathrm{s}}\boldsymbol{\mathcal{E}}_y(\mathbf{u}_\pi)) = 0 \quad \text{in } Y_{\mathrm{s}},\\
\tilde{\varepsilon}\tilde{\varepsilon}_0\boldsymbol{E}\cdot\boldsymbol{n} = -\sigma \quad \text{on } \partial Y_{\mathrm{fs}} & (\boldsymbol{c}_{\mathrm{s}}\boldsymbol{\mathcal{E}}_y(\mathbf{u}_\pi))\boldsymbol{n} = -\boldsymbol{\Pi}_{\mathrm{d}}\boldsymbol{n} \quad \text{on } \partial Y_{\mathrm{fs}},
\end{array}
\tag{2.5}
$$

with $\sigma < 0$ denoting the fixed surface charge and $\boldsymbol{n}$ the unit normal exterior to Y_{f}. The effective coefficients admit the following microscopic representations

$$
\begin{aligned}
&\boldsymbol{\Pi} = \langle\boldsymbol{\Pi}_{\mathrm{d}}\rangle + n_{\mathrm{s}}\boldsymbol{\Pi}_{\mathrm{S}}, \quad \boldsymbol{\Pi}_S = -\langle\boldsymbol{c}_{\mathrm{s}}\boldsymbol{\mathcal{E}}_y(\mathbf{u}_\pi)\rangle^{\mathrm{s}}, \quad \boldsymbol{C}_{\mathrm{s}} = \langle\boldsymbol{c}_s(\boldsymbol{II} + \boldsymbol{\mathcal{E}}_y(\boldsymbol{\xi}))\rangle,\\
&\boldsymbol{\alpha} = n_{\mathrm{f}}\boldsymbol{I} - \langle\boldsymbol{c}_{\mathrm{s}}\boldsymbol{\mathcal{E}}_y(\boldsymbol{\zeta})\rangle = n_{\mathrm{f}}\boldsymbol{I} - \langle\nabla_y\cdot\boldsymbol{\xi}\rangle, \quad \beta = \langle\nabla_y\cdot\boldsymbol{\zeta}\rangle,\\
&\boldsymbol{K}_{\mathrm{P}} = \langle\boldsymbol{\kappa}_{\mathrm{p}}\rangle, \quad \boldsymbol{K}_{\mathrm{C}} = \langle\boldsymbol{\kappa}_{\mathrm{c}}\rangle, \quad \boldsymbol{K}_{\mathrm{E}} = \langle\boldsymbol{\kappa}_{\mathrm{e}}\rangle,\\
&\boldsymbol{D}_{\pm}^{\boldsymbol{I}} = \mathcal{D}_{\pm}\left\langle\exp(\mp\bar{\varphi})\left(\boldsymbol{I} + \nabla_y\boldsymbol{f}^{\pm} + c_{\mathrm{b}}\nabla_y\boldsymbol{h}_I^{\pm}\right)\right\rangle^{\mathrm{f}},\\
&\boldsymbol{D}_{\pm}^{\mathrm{p}} = \mathcal{D}_{\pm}c_{\mathrm{b}}\left\langle\exp(\mp\bar{\varphi})\nabla_y\boldsymbol{h}_{\mathrm{p}}^{\pm}\right\rangle^{\mathrm{f}}, \quad \boldsymbol{I} = \mathrm{c}, \mathrm{e},\\
&\gamma_\pi = \langle\nabla_y\cdot\mathbf{u}_\pi\rangle, \quad G_\pm\mathbf{v}_\pm = \langle\exp(\mp\bar{\varphi})\mathbf{v}\rangle, \quad G_\pm = \langle\exp(\mp\bar{\varphi})\rangle^{\mathrm{f}}.
\end{aligned}
\tag{2.6}
$$

Here $\boldsymbol{\xi}$ denotes a, third-order characteristic tensor and $\{\boldsymbol{\zeta}, \boldsymbol{f}^{\pm}\}$ a pair of vectorial characteristic functions satisfying the canonical cell problems

$$
\begin{array}{ll|ll}
\nabla_y\cdot(\boldsymbol{c}_{\mathrm{s}}\boldsymbol{\mathcal{E}}_y(\boldsymbol{\xi})) = 0 \quad \text{in } Y_{\mathrm{s}}, & & \nabla_y\cdot(\boldsymbol{c}_{\mathrm{s}}\boldsymbol{\mathcal{E}}_y(\boldsymbol{\zeta})) = 0 \quad \text{in } Y_{\mathrm{s}}, & \\
(\boldsymbol{c}_{\mathrm{s}}\boldsymbol{\mathcal{E}}_y(\boldsymbol{\xi}))\boldsymbol{n} = -\boldsymbol{c}_{\mathrm{s}}\boldsymbol{I}\boldsymbol{I}n \quad \text{on } \partial Y_{fs}, & & (\boldsymbol{c}_{\mathrm{s}}\boldsymbol{\mathcal{E}}_y(\boldsymbol{\zeta}))\boldsymbol{n} = -\boldsymbol{I}\boldsymbol{n} \quad \text{on } \partial Y_{\mathrm{fs}} &
\end{array}
\tag{2.7}
$$

and

$$
\begin{aligned}
&\nabla_y\cdot\left(\mathcal{D}_{\pm}\exp(\mp\bar{\varphi})\nabla_y\boldsymbol{f}^{\pm}\right) = \pm\boldsymbol{I}\mathcal{D}_{\pm}\exp(\pm\bar{\varphi})\nabla_y\bar{\varphi} \text{ in } Y_{\mathrm{f}},\\
&\nabla_y\boldsymbol{f}^{\pm}\cdot\boldsymbol{n} = \mp\mathbf{I}\mathbf{n} \quad \text{on } \partial Y_{\mathrm{fs}}.
\end{aligned}
\tag{2.8}
$$

In addition, $\boldsymbol{\kappa}_I$ and $\boldsymbol{h}_I^{\pm}(I = \mathrm{p}, \mathrm{c}, \mathrm{e})$ denote other characteristic functions associated with the fluid flow, whose vectorial and scalar components $\boldsymbol{\kappa}_I^{\mathrm{j}}$ and $h_I^{\pm j}(\mathrm{j} = 1, 2, 3)$, together with the pressures g_I^{j} satisfy the extended Stokes problems

$$
\begin{aligned}
&\mu_{\mathrm{f}}\Delta_{yy}\boldsymbol{\kappa}_{\mathrm{p}}^{\mathrm{j}}-\nabla_y g_{\mathrm{p}}^{\mathrm{j}}-A\nabla_y h_{\mathrm{p}}^{+\mathrm{j}}-B\nabla_y h_{\mathrm{p}}^{-\mathrm{j}}=-\boldsymbol{e}^{\mathrm{j}}\quad\text{in } Y_{\mathrm{f}},\\
&\nabla_y\cdot\boldsymbol{\kappa}_{\mathrm{p}}^{\mathrm{j}}=0,\quad \mathrm{j}=1,2,3,\\
&\nabla_y\cdot\left[\mathcal{D}_{\pm}\exp(\mp\bar{\varphi})\nabla_y h_{\mathrm{p}}^{\pm j}\right]\pm\boldsymbol{\kappa}_{\mathrm{p}}^{\mathrm{j}}\cdot(\exp(\mp\bar{\varphi})\nabla_y\bar{\varphi}=0,\\
&\boldsymbol{\kappa}_{\mathrm{p}}^{\mathrm{j}}=0;\quad \nabla_y h_{\mathrm{p}}^{\pm j}\cdot\boldsymbol{n}=0\quad\text{on } \partial Y_{\mathrm{fs}}
\end{aligned}
\tag{2.9}
$$

and

$$
\begin{aligned}
&\mu_{\mathrm{f}}\Delta_{yy}\boldsymbol{\kappa}_{\mathrm{c}}^{\mathrm{j}}-\nabla_y g_{\mathrm{c}}^{\mathrm{j}}-A\nabla_y h_{\mathrm{c}}^{+\mathrm{j}}-B\nabla_y h_{\mathrm{c}}^{-\mathrm{j}}=-\boldsymbol{F}\boldsymbol{e}^{\mathrm{j}}\quad\text{in } Y_{\mathrm{f}},\\
&\nabla_y\cdot\boldsymbol{\kappa}_{\mathrm{c}}^{\mathrm{j}}=0,\quad \mathrm{j}=1,2,3,\\
&\nabla_y\cdot\left[\mathcal{D}_{\pm}\exp(\mp\bar{\varphi})\nabla_y h_{\mathrm{c}}^{\pm j}\right]\pm\boldsymbol{\kappa}_{\mathrm{c}}^{\mathrm{j}}\cdot(\exp(\mp\bar{\varphi})\nabla_y\bar{\varphi}=0,\\
&\boldsymbol{\kappa}_{\mathrm{c}}^{\mathrm{j}}=0,\quad \nabla_y h_{\mathrm{c}}^{\pm j}\cdot\boldsymbol{n}=0\quad\text{on } \partial Y_{\mathrm{fs}}
\end{aligned}
\tag{2.10}
$$

along with

$$
\begin{aligned}
&\mu_{\mathrm{f}}\Delta_{yy}\boldsymbol{\kappa}_{\mathrm{e}}^{\mathrm{j}}-\nabla_y g_{\mathrm{e}}^{\mathrm{j}}-A\nabla_y h_{\mathrm{e}}^{+\mathrm{j}}-B\nabla_y h_{\mathrm{e}}^{-\mathrm{j}}=-\boldsymbol{G}\boldsymbol{e}^{\mathrm{j}}\quad\text{in } Y_{\mathrm{f}},\\
&\nabla_y\cdot\boldsymbol{\kappa}_{\mathrm{e}}^{\mathrm{j}}=0,\quad \mathrm{j}=1,2,3,\\
&\nabla_y\cdot\left[\mathcal{D}_{\pm}\exp(\mp\bar{\varphi})\nabla_y h_{\mathrm{e}}^{\pm j}\right]\pm\boldsymbol{\kappa}_{\mathrm{e}}^{\mathrm{j}}\cdot(\exp(\mp\bar{\varphi})\nabla_y\bar{\varphi}=0,\\
&\boldsymbol{\kappa}_{\mathrm{e}}^{\mathrm{j}}=0;\quad \nabla_y h_{\mathrm{e}}^{\pm j}\cdot\boldsymbol{n}=0\quad\text{on } \partial Y_{\mathrm{fs}},
\end{aligned}
\tag{2.11}
$$

where

$$
\begin{aligned}
&\boldsymbol{F}=RT\left[2(\cosh\bar{\varphi}-1)\boldsymbol{I}+(\exp(-\bar{\varphi})-1)\nabla_y\boldsymbol{f}^{+}+(\exp(+\bar{\varphi})-1)\nabla_y\boldsymbol{f}^{-}\right],\\
&\boldsymbol{G}=RTc_{\mathrm{b}}\left[-2\sinh\bar{\varphi}\boldsymbol{I}-(\exp(-\bar{\varphi})-1)\nabla_y\boldsymbol{f}^{+}-(\exp(+\bar{\varphi})-1)\nabla_y\boldsymbol{f}^{-}\right],\\
&\boldsymbol{A}=RTc_{\mathrm{b}}[\exp(-\bar{\varphi})-1],\quad B=RTc_{\mathrm{b}}[\exp(+\bar{\varphi})-1].
\end{aligned}
\tag{2.12}
$$

The coefficients $\{\boldsymbol{\xi},\boldsymbol{\zeta}\}$ in (2.7) are purely geometrical quantities only depending on cell morphology whereas the functions $\left\{\boldsymbol{f}^{\pm},\boldsymbol{\kappa}_I,\boldsymbol{h}_I^{\pm}\right\}$ ($I=$ p, c, e) in (2.8)–(2.11) are strongly dictated by the e.d.l. potential $\bar{\varphi}$, solution of the Poisson–Boltzmann problem (2.5)(a) and consequently depend on the bulk concentration c_{b}, through the definition of the Debye's length ℓ_{D}. It should be noted that the dependence of $\boldsymbol{f}^{\pm}$ on c_{b} is inherent to charged species and does not appear in the homogenization of convection-diffusion equations of nonionic species for the Peclet number of $\mathcal{O}(1)$ (see Auriault and Adler, 1995).

The cation and anion concentrations c_+ and c_- are related to the bulk concentration c_b and the relative e.d.l. potential through the generalized Boltzmann distributions $c_{\pm}=c_{\mathrm{b}}\exp(\mp\bar{\varphi})$. This implies the net charge density given by $q=F(c_+-c_-)=-2Fc_{\mathrm{b}}\sinh\bar{\varphi}$ and its macroscopic counterpart $q_*\equiv\langle q\rangle=F(c_+-c_-)=-2Fc_{\mathrm{b}}\langle\sinh\bar{\varphi}\rangle$. Further, denoting $\langle\sigma\rangle^{\mathrm{fs}}=|\partial Y_{\mathrm{fs}}|^{-1}\int_{\partial Y_{\mathrm{fs}}}\sigma\,\mathrm{d}Y$ the interfacial averaging of the surface charge and

$n_{\mathrm{fs}} = |\partial Y_{\mathrm{fs}}|/|Y|$ the surface volume fraction, the compatibility condition between the Neumann boundary condition and the source term in the Poisson–Boltzmann problem (2.5)(a) leads to the electroneutrality condition

$$\frac{1}{|Y|}\int_{\partial Y_{\mathrm{fs}}} \sigma \,\mathrm{d}\Gamma = n_{\mathrm{fs}}\langle\sigma\rangle^{\mathrm{fs}} = \frac{\tilde{\varepsilon}\tilde{\varepsilon}_0 RT}{F|Y|}\int_{\partial Y_{\mathrm{fs}}} \nabla_y\bar{\varphi}\cdot\boldsymbol{n}\,\mathrm{d}\Gamma = \frac{\tilde{\varepsilon}\tilde{\varepsilon}_0 RT}{F|Y|}\int_{Y_{\mathrm{f}}} \Delta_{yy}\bar{\varphi}\,\mathrm{d}Y$$
$$= 2Fc_{\mathrm{b}}\langle\sinh\bar{\varphi}\rangle = -q_*. \tag{2.13}$$

The above system is supplemented by macroscopic initial and boundary conditions on the macroscopic boundary of the swelling medium. Finally, we remark that the set of variables $\{p_{\mathrm{b}}, c_{\mathrm{b}}, \bar{\psi}_{\mathrm{b}}\}$, whose gradients are the driving forces for fluid flow, are associated with an apparent bulk fluid characterized by the absence of a net charge density and the fulfillment of the electroneutrality pointwisely. In the fictitious liquid the suspended species at hidden concentration $c_{\mathrm{b}+} = c_{\mathrm{b}-} = c_{\mathrm{b}}$ are constructed at local equilibrium with the ions such that their electro-chemical potential are equal. After solving for these variables and for the local e.d.l. potential $\bar{\varphi}$, the intrinsic averaging of the ion concentrations, total dimensionless electric potential and fluid pressure, $\langle c_{\pm}\rangle^{\mathrm{f}}, \langle\bar{\Phi}\rangle^{\mathrm{f}}, \langle p\rangle^{\mathrm{f}}$ can be computed in a post-processing approach using the relations (see Moyne and Murad (2006) for details)

$$\langle c_{\pm}\rangle^{\mathrm{f}} = c_{\mathrm{b}}\langle\exp(\mp\bar{\varphi})\rangle^{\mathrm{f}}, \quad \langle\bar{\Phi}\rangle^{\mathrm{f}} = \langle\bar{\varphi}\rangle^{\mathrm{f}} + \bar{\psi}_{\mathrm{b}},$$
$$\langle p\rangle^{\mathrm{f}} = \langle p_b + \pi\rangle^{\mathrm{f}} = p_{\mathrm{b}} + 2RTc_{\mathrm{b}}(\langle\cosh\bar{\varphi}\rangle^{\mathrm{f}} - 1) = p_{\mathrm{b}} + RT(\langle c_+ + c_-\rangle^{\mathrm{f}} - 2c_{\mathrm{b}}).$$

2.2. SUMMARY OF THE ALTERNATIVE FORMULATION BASED ON ONSAGER'S RECIPROCITY RELATIONS

The two-scale formulation can also be rephrased in terms of alternative variables, which naturally embed the macroscopic model in the framework of the Thermodynamics of Irreversible Processes and Onsager's reciprocity relations. To this end we begin by replacing the dimensionless potential $\bar{\psi}_{\mathrm{b}}$ by the electric potential $\psi_{\mathrm{b}} = RT\bar{\psi}_{\mathrm{b}}/F$ and concentration c_{b} by the bulk chemical potential of the species (or the Nernst potential) $\mu_{\mathrm{b}} = RT\ln c_{\mathrm{b}}$). Associated with the thermodynamic driving forces $\{\nabla_{p_{\mathrm{b}}}, \nabla_{\mu_{\mathrm{b}}}, \nabla_{\psi_{\mathrm{b}}}\}$ we define the conjugated fluxes consisting of the total flux of species relative to the advection induced by the Darcy's velocity $\boldsymbol{J}_{\mathrm{c}}$, the electric current $\boldsymbol{I}_{\mathrm{e}}$, the overall and excess electrical capacities $\{G_{\mathrm{c}}, G_{\mathrm{s}}\}$, the overall and relative advection velocities $\{\mathbf{v}_{\mathrm{c}}, \mathbf{v}_{\mathrm{s}}\}$ and the overall and excess diffusion coefficients $\{\boldsymbol{D}_*^I, \boldsymbol{\Delta}_*^I\}$. We then have the definitions

$$
\begin{aligned}
&\boldsymbol{J}_{\mathrm{c}} \equiv \boldsymbol{J}_{+} + \boldsymbol{J}_{-} - n_f G_c c_{\mathrm{b}} \frac{\partial \mathbf{u}}{\partial t} - 2c_{\mathrm{b}} \mathbf{v}_{\mathrm{D}}, \quad \boldsymbol{I}_{\mathrm{e}} \equiv F(\boldsymbol{J}_{+} - J_{-}) - n_f G_s c_{\mathrm{b}} \frac{\partial \mathbf{u}}{\partial t}, \\
&G_{\mathrm{c}} \equiv G_{+} + G_{-} = 2\langle \cosh \bar{\varphi} \rangle^{\mathrm{f}}, \quad G_{\mathrm{s}} \equiv G_{+} - G_{-} = -2\langle \sinh \bar{\varphi} \rangle^{\mathrm{f}}, \\
&G_{\mathrm{c}} \mathbf{v}_{ch} \equiv G_{+} \left(\mathbf{v}_{+} - n_f \frac{\partial \mathbf{u}}{\partial t} \right) + G_{-} \left(\mathbf{v}_{-} - n_f \frac{\partial \mathbf{u}}{\partial t} \right) = 2 \left\langle \cosh \bar{\varphi} \left(\mathbf{v} - \frac{\partial \mathbf{u}}{\partial t} \right) \right\rangle; \\
&G_s \mathbf{v}_{sh} \equiv G_{+} \left(\mathbf{v}_{+} - n_f \frac{\partial \mathbf{u}}{\partial t} \right) - G_{-} \left(\mathbf{v}_{-} - n_f \frac{\partial \mathbf{u}}{\partial t} \right).
\end{aligned} \tag{2.14}
$$

By adding and subtracting the mass balances in (2.2) over cations and anions and using the last step in (2.13) we obtain the Overall mass conservation of the species and electric charge

$$
\begin{aligned}
&\frac{\partial}{\partial t}(n_f G_{\mathrm{c}} c_{\mathrm{b}}) + \nabla_x \cdot \left(2c_{\mathrm{b}} \mathbf{v}_D + n_f G_c c_b \frac{\partial \mathbf{u}}{\partial t} \right) = -\nabla_x \cdot \boldsymbol{J}_d, \\
&F \frac{\partial}{\partial t}(n_f G_{\mathrm{s}} c_{\mathrm{b}}) = \frac{\partial q_*}{\partial t} = -\nabla \cdot \left(\boldsymbol{I}_{\mathrm{e}} + F n_f G_s c_b \frac{\partial \mathbf{u}}{\partial t} \right).
\end{aligned} \tag{2.15}
$$

The constitutive laws for $\{\boldsymbol{J}_{\mathrm{c}}, \boldsymbol{J}_{\mathrm{e}}\}$ are obtained by further manipulating the Nernst–Planck relations (2.3) yielding

$$
\boldsymbol{J}_{\mathrm{c}} = c_{\mathrm{b}}(G_{\mathrm{c}} \mathbf{v}_{\mathrm{c}} - 2\mathbf{v}_D) - n_{\mathrm{f}}(\boldsymbol{D}_*^{\mathrm{c}} \nabla_x c_{\mathrm{b}} + \boldsymbol{\Delta}_*^{\mathrm{e}} c_{\mathrm{b}} \nabla_x \overline{\psi}_{\mathrm{b}} + \boldsymbol{D}_*^{p} \nabla_x p_{\mathrm{b}}), \tag{2.16}
$$

$$
\boldsymbol{I}_{\mathrm{e}} = F c_{\mathrm{b}} G_{\mathrm{s}} \mathbf{v}_{\mathrm{s}} - n_{\mathrm{f}} F(\boldsymbol{\Delta}_*^{\mathrm{c}} \nabla_x c_{\mathrm{b}} + \boldsymbol{D}_*^{\mathrm{e}} c_{\mathrm{b}} \nabla_x \overline{\psi}_{\mathrm{b}} + \boldsymbol{\Delta}_*^{p} \nabla_x p_{\mathrm{b}}), \tag{2.17}
$$

where using the microscopic representation for $G_{\mathrm{c}} \mathbf{v}_{\mathrm{c}}$ and $G_{\mathrm{s}} \mathbf{v}_{\mathrm{s}}$ in (2.14) and the local decomposition for $\mathbf{v}$ in (2.4) give

$$
G_{\mathrm{c}} \mathbf{v}_{\mathrm{c}} = -2\langle \cosh \overline{\varphi} \kappa_{\mathrm{p}} \rangle \nabla p_{\mathrm{b}} - 2\langle \cosh \overline{\varphi} \kappa_{\mathrm{c}} \rangle \nabla c_{\mathrm{b}} - 2\langle \cosh \overline{\varphi} \kappa_{\mathrm{e}} \rangle \nabla \overline{\psi}_{\mathrm{b}}, \tag{2.18}
$$

$$
G_{\mathrm{s}} \mathbf{v}_{\mathrm{s}} = 2\langle \sinh \overline{\varphi} \kappa_{\mathrm{p}} \rangle \nabla p_{\mathrm{b}} + 2\langle \sinh \overline{\varphi} \kappa_{\mathrm{c}} \rangle \nabla c_{\mathrm{b}} + 2\langle \sinh \overline{\varphi} \kappa_{\mathrm{e}} \rangle \nabla \overline{\psi}_{\mathrm{b}}. \tag{2.19}
$$

Thus, combining (2.16) and (2.17) with Darcy's law (2.1) and also making use of (2.18) and (2.19) we obtain the fluxes $\{\mathbf{v}_D, \boldsymbol{J}_{\mathrm{c}}, \boldsymbol{I}_{\mathrm{e}}\}$ conjugated (in the thermodynamical sense) with the driving forces $\{\nabla_x p_{\mathrm{b}}, \nabla_x \mu_{\mathrm{b}}, \nabla_x \psi_{\mathrm{b}}\}$ through Onsager's reciprocity relations

$$
\begin{aligned}
\mathbf{v}_{\mathrm{D}} &= -\boldsymbol{L}_{\mathrm{PP}} \nabla_x p_{\mathrm{b}} - \boldsymbol{L}_{\mathrm{PC}} RT \nabla_x \ln c_{\mathrm{b}} - \boldsymbol{L}_{\mathrm{PE}} \nabla_x \psi_{\mathrm{b}}, \\
\boldsymbol{J}_{\mathrm{c}} &= -\boldsymbol{L}_{\mathrm{CP}} \nabla_x p_{\mathrm{b}} - \boldsymbol{L}_{\mathrm{CC}} RT \nabla_x \ln c_{\mathrm{b}} - \boldsymbol{L}_{\mathrm{CE}} \nabla_x \psi_{\mathrm{b}}, \\
\boldsymbol{I}_{\mathrm{e}} &= -\boldsymbol{L}_{\mathrm{EP}} \nabla_x p_{\mathrm{b}} - \boldsymbol{L}_{\mathrm{EC}} RT \nabla_x \ln c_{\mathrm{b}} - \boldsymbol{L}_{\mathrm{EE}} \nabla_x \psi_{\mathrm{b}}
\end{aligned} \tag{2.20}
$$

with the Onsager's coefficients $\boldsymbol{L}_{\mathrm{IJ}} (I, J = P, C, E)$ microscopically represented as

$$
\begin{aligned}
&\boldsymbol{L}_{\mathrm{PP}}=\boldsymbol{K}_{\mathrm{P}},\quad \boldsymbol{L}_{\mathrm{PC}}=\frac{c_{\mathrm{b}}\boldsymbol{K}_{\mathrm{C}}}{RT},\quad \boldsymbol{L}_{\mathrm{PE}}=\frac{F\boldsymbol{K}_{\mathrm{E}}}{RT},\\
&\boldsymbol{L}_{\mathrm{CP}}=\left(2c_{\mathrm{b}}\langle\boldsymbol{\kappa}_{\mathrm{p}}(\cosh\overline{\varphi}-1)\rangle+n_{\mathrm{f}}\boldsymbol{D}_{*}^{\mathrm{p}}\right),\\
&\boldsymbol{L}_{\mathrm{CC}}=\frac{c_{\mathrm{b}}}{RT}\left(2c_{\mathrm{b}}\langle\boldsymbol{\kappa}_{\mathrm{c}}(\cosh\overline{\varphi}-1)\rangle+n_{\mathrm{f}}\boldsymbol{D}_{*}^{\mathrm{c}}\right),\\
&\boldsymbol{L}_{\mathrm{CE}}=\frac{Fc_{\mathrm{b}}}{RT}\left(2\langle\boldsymbol{\kappa}_{\mathrm{e}}(\cosh\overline{\varphi}-1)\rangle+n_{\mathrm{f}}\boldsymbol{\Delta}_{*}^{\mathrm{e}}\right),\quad \boldsymbol{L}_{\mathrm{EP}}=F\left(-2c_{\mathrm{b}}\langle\boldsymbol{\kappa}_{\mathrm{p}}\sinh\overline{\varphi}\rangle+n_{\mathrm{f}}\boldsymbol{\Delta}_{*}^{\mathrm{p}}\right),\\
&\boldsymbol{L}_{\mathrm{EC}}=\frac{Fc_{\mathrm{b}}}{RT}\left(-2c_{\mathrm{b}}\langle\boldsymbol{\kappa}_{\mathrm{c}}\sinh\overline{\varphi}\rangle+n_{\mathrm{f}}\boldsymbol{\Delta}_{*}^{\mathrm{c}}\right),\quad \boldsymbol{L}_{\mathrm{EE}}=\frac{F^2c_{\mathrm{b}}}{RT}\left(-2\langle\boldsymbol{\kappa}_{\mathrm{e}}\sinh\overline{\varphi}\rangle+n_{\mathrm{f}}\boldsymbol{D}_{*}^{\mathrm{e}}\right).
\end{aligned}
\tag{2.21}
$$

Finally an alternative form of the eletroneutrality condition can be derived. Using (2.13) in (2.15) we obtain

$$
\frac{\partial}{\partial t}(n_{\mathrm{fs}}\langle\sigma\rangle^{\mathrm{fs}})-\nabla_x\cdot\left(\boldsymbol{I}_{\mathrm{e}}+n_{\mathrm{f}}G_{\mathrm{s}}c_{\mathrm{b}}\frac{\partial\mathbf{u}}{\partial t}\right)=0
$$

in which when combined with (2.13), the definition for G_s in (2.14) and the conservation of charge in the solid phase (see Gray and Hassanizadeh, 1989; Hassanizadeh and Gray, 1990)

$$
\frac{\partial}{\partial t}\left(n_{\mathrm{fs}}\langle\sigma\rangle^{\mathrm{fs}}\right)+\nabla_x\left(n_{\mathrm{fs}}\langle\sigma\rangle^{\mathrm{fs}}\frac{\partial\mathbf{u}}{\partial t}\right)=0
$$

furnish

$$
\nabla_x.\left(\boldsymbol{I}_{\mathrm{e}}+(Fn_{\mathrm{f}}G_{\mathrm{s}}c_{\mathrm{b}}+n_{\mathrm{fs}}\langle\sigma\rangle^{\mathrm{fs}})\frac{\partial\mathbf{u}}{\partial t}\right)=\nabla_x.\boldsymbol{I}_{\mathrm{e}}=0.
\tag{2.22}
$$

The above form of the electroneutrality condition shows conservation of the net charge flux in a reference frame moving together with the solid phase.

Our alternative two-scale model can be stated in the following manner: Find the Macroscopic unknowns $\{\boldsymbol{\sigma}_T,\mathbf{u},n_{\mathrm{f}},p_{\mathrm{b}},c_{\mathrm{b}},\psi_{\mathrm{b}},\mathbf{v}_{\mathrm{D}},\boldsymbol{J}_{\mathrm{c}},\boldsymbol{I}_{\mathrm{e}}\}$ satisfying

$$
\begin{aligned}
&\nabla_x.\boldsymbol{\sigma}_T=0,\\
&\boldsymbol{\sigma}_T=-\boldsymbol{\alpha}p_{\mathrm{b}}+\boldsymbol{C}_{\mathrm{s}}\boldsymbol{\mathcal{E}}_x(\mathbf{u})-\Pi,\\
&\nabla_x.\mathbf{v}_{\mathrm{D}}+\boldsymbol{\alpha}:\frac{\partial}{\partial t}\boldsymbol{\mathcal{E}}_x(\mathbf{u})=\beta\frac{\partial p_{\mathrm{b}}}{\partial t}+\frac{\partial\gamma_\pi}{\partial t},\\
&\frac{\partial n_{\mathrm{f}}}{\partial t}+\nabla_x.\mathbf{v}_{\mathrm{D}}+n_{\mathrm{f}}\nabla_x.\frac{\partial\mathbf{u}}{\partial t}=0,\\
&\begin{cases}\dfrac{\partial}{\partial t}(n_{\mathrm{f}}G_{\mathrm{c}}c_{\mathrm{b}})+\nabla_x.(2c_{\mathrm{b}}\mathbf{v}_D+n_{\mathrm{f}}G_{\mathrm{c}}c_{\mathrm{b}}\dfrac{\partial\mathbf{u}}{\partial t}+J_{\mathrm{d}})=0,\\ \nabla_x.\boldsymbol{I}_{\mathrm{e}}=0\quad\text{in }\Omega,\end{cases}\\
&\mathbf{v}_{\mathrm{D}}=-\boldsymbol{L}_{\mathrm{PP}}\nabla_x p_{\mathrm{b}}-\boldsymbol{L}_{\mathrm{PC}}RT\nabla_x\ln c_{\mathrm{b}}-\boldsymbol{L}_{\mathrm{PE}}\nabla_x\psi_{\mathrm{b}},\\
&\boldsymbol{J}_{\mathrm{c}}=-\boldsymbol{L}_{\mathrm{CP}}\nabla_x p_{\mathrm{b}}-\boldsymbol{L}_{\mathrm{CC}}RT\nabla_x\ln c_{\mathrm{b}}-\boldsymbol{L}_{\mathrm{CE}}\nabla_x\psi_{\mathrm{b}},\\
&\boldsymbol{I}_{\mathrm{e}}=-\boldsymbol{L}_{\mathrm{EP}}\nabla_x p_{\mathrm{b}}-\boldsymbol{L}_{\mathrm{EC}}RT\nabla_x\ln c_{\mathrm{b}}-\boldsymbol{L}_{\mathrm{EE}}\nabla_x\psi_{\mathrm{b}},
\end{aligned}
$$

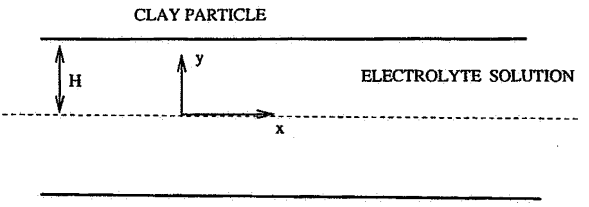

Figure 1. Unit cell geometry of two parallel clay particles in a highly compacted clay.

where the parameters $\{\boldsymbol{\alpha}, \boldsymbol{C}_s, \boldsymbol{\Pi}, \beta, \gamma_\pi\}$ and $\{G_c, G_s\}$ admit the microscopic representations in (2.6) and (2.14) and the Onsager's coefficients $\boldsymbol{L}_{IJ}(I, J = P, C, E\}$ are microscopically represented by (2.21).

3. Application to Stratified Microstructures

We shall henceforth discuss the application of the two-scale formulation to the case of highly compacted clays with microstructure composed of parallel particles of face-to-face contact (Figure 1). We concentrate our discussion on a single unit cell ($\boldsymbol{x} = \text{cte}$) where we associate a local rectangular coordinate system $\boldsymbol{y} = \{x, y\}$ with an orthogonal basis $\{\boldsymbol{e}^1, \boldsymbol{e}^2\}$ of unitary vectors parallel and normal to the particle surface. In this microscopic picture, the flow of the electrolyte solution and transport of the ions take place in the axial x-direction (parallel to $\boldsymbol{e}^1$) whereas the e.d.l. potential $\overline{\varphi}$ varies in the y-direction normal to the particle surface (parallel to $\boldsymbol{e}^2$). As we shall illustrate next, in this particular arrangement the complexity inherent to the closure problems is somewhat reduced.

3.1. REDUCED CLOSURE PROBLEMS

Hereafter we represent the aforementioned closure problems in the rectangular coordinate system of Figure 1. Begin by denoting the scalar transversal component of the local electric field by E, and also designate $\kappa_I (I = \text{p, c, e})$ the axial components of the characteristic velocities κ_I^{j} with $\text{j} = 1$, and v the axial component of the liquid velocity $\mathbf{v}$. By invoking (2.4) and (2.5)(a), the reduced two-dimensional representations of the fluid stress $\boldsymbol{\sigma}_f$, Maxwell stress $\boldsymbol{\tau}_M$ and disjoining tensor $\boldsymbol{\Pi}_d$, along with the uni-dimensional representations of E and v read as

$$E = -\frac{RT}{F}\frac{\partial \overline{\varphi}}{\mathrm{d}y}, \tag{3.1}$$

$$v = -\kappa_p \frac{\partial p_b}{\partial x} - \kappa_c \frac{\partial c_b}{\partial x} - \kappa_e \frac{\partial \bar{\psi}_b}{\partial x}, \tag{3.2}$$

$$\boldsymbol{\tau}_{\boldsymbol{M}} = \frac{\tilde{\varepsilon}\tilde{\varepsilon}_0}{2}\left(E^2\boldsymbol{e}^2\otimes\boldsymbol{e}^2 - E^2\boldsymbol{e}^1\otimes\boldsymbol{e}^1\right),$$
$$\boldsymbol{\sigma}_{\mathrm{f}} = -p_t\boldsymbol{e}^1\otimes\boldsymbol{e}^1 - p_n\boldsymbol{e}^2\otimes\boldsymbol{e}^2, \tag{3.3}$$

$$\boldsymbol{\Pi}_{\mathrm{d}} = \Pi_{\mathrm{d}}\boldsymbol{e}^2\otimes\boldsymbol{e}^2 + \left(\pi + \frac{\tilde{\varepsilon}\tilde{\varepsilon}_0}{2}E^2\right)\boldsymbol{e}^1\otimes\boldsymbol{e}^1$$
$$= \Pi_{\mathrm{d}}\boldsymbol{e}^2\otimes\boldsymbol{e}^2 + \left(\Pi_{\mathrm{d}} + \tilde{\varepsilon}\tilde{\varepsilon}_0E^2\right)\boldsymbol{e}^1\otimes\boldsymbol{e}^1,$$

where the component $\Pi_{\mathrm{d}} \equiv \boldsymbol{\Pi}_{\mathrm{d}}\boldsymbol{e}^2\cdot\boldsymbol{e}^2$ normal to the surface denotes the disjoining pressure in the sense of Derjaguin *et al.* (1987) and p_{n} and p_{t} are the normal and tangential components of $\boldsymbol{\sigma}_{\mathrm{f}}$ given by

$$\Pi_{\mathrm{d}} = \pi - \frac{\tilde{\varepsilon}\tilde{\varepsilon}_0}{2}E^2 = 2RTc_{\mathrm{b}}(\cosh\bar{\varphi} - 1) - \frac{\tilde{\varepsilon}\tilde{\varepsilon}_0}{2}E^2, \tag{3.4}$$
$$p_{\mathrm{n}} = p_{\mathrm{b}} + \Pi_{\mathrm{d}}, \quad p_{\mathrm{t}} = p_{\mathrm{b}} + \Pi_{\mathrm{d}} + \tilde{\varepsilon}\tilde{\varepsilon}E^2. \tag{3.5}$$

Since the stress state in the electrolyte solution is anisotropic one may introduce the deviatoric part of $\boldsymbol{\sigma}_{\mathrm{f}}$. Using (3.5) in (3.3) the two-dimensional representation for this quantity reads as

$$\boldsymbol{S} \equiv \boldsymbol{\sigma}_{\mathrm{f}} - \tfrac{1}{2}\mathrm{tr}\boldsymbol{\sigma}_{\mathrm{f}}\boldsymbol{I} = \boldsymbol{\sigma}_{\mathrm{f}} + \tfrac{1}{2}(p_{\mathrm{t}} + p_{\mathrm{n}})\boldsymbol{I} = \boldsymbol{\sigma}_{\mathrm{f}} + \left(p_{\mathrm{d}} + \Pi_{\mathrm{d}} + \frac{\tilde{\varepsilon}\tilde{\varepsilon}_0}{2}E^2\right)\boldsymbol{I}$$
$$= -\frac{\tilde{\varepsilon}\tilde{\varepsilon}_0}{2}E^2\boldsymbol{e}^1\otimes\boldsymbol{e}^1 + \frac{\tilde{\varepsilon}\tilde{\varepsilon}_0}{2}E^2\boldsymbol{e}^2\otimes\boldsymbol{e}^2 = \frac{\tilde{\varepsilon}\tilde{\varepsilon}_0E^2}{2}(\boldsymbol{e}^2\otimes\boldsymbol{e}^2 - \boldsymbol{e}^1\otimes\boldsymbol{e}^1). \tag{3.6}$$

We now consider the local e.d.l. potential distribution. To this end we note that the periodicity in the x-direction together with the fact that σ is constant allow to reduce the Poisson Boltzmann equation (2.5) (a) to a one-dimensional problem in the transversal direction. We then have

$$\tilde{\varepsilon}_0\tilde{\varepsilon}\frac{\mathrm{d}^2\bar{\varphi}}{\mathrm{d}y^2} = \frac{2F^2c_{\mathrm{b}}}{RT}\sinh\bar{\varphi}, \qquad E = -\frac{RT}{F}\frac{\mathrm{d}\bar{\varphi}}{\mathrm{d}y},$$
$$\frac{\mathrm{d}\bar{\varphi}}{\mathrm{d}y} = 0 \quad \text{at } y = 0,$$
$$E = -\frac{\sigma}{\tilde{\varepsilon}\tilde{\varepsilon}_0} \quad \text{at } y = H, \tag{3.7}$$

which leads to the reduced distribution $\bar{\varphi} = \bar{\varphi}(y)$ parametrized by the pair $\{c_{\mathrm{b}}, H\}$.

Now consider the reduced version of the closure problems (2.7)–(2.11). Begin by replacing $\nabla_y\bar{\varphi}$ by its nonzero component $(\mathrm{d}\bar{\varphi}/\mathrm{d}y)\boldsymbol{e}^2$ and denote $\boldsymbol{f}_{\mathrm{j}}^{\pm}$ the component of $\boldsymbol{f}^{\pm}$ obtained by replacing $\boldsymbol{I}$ by $\boldsymbol{e}^{\mathrm{j}}$ in (2.8). The closure problems for $\{f_1^{\pm}, f_2^{\pm}\}$ are given by

$$\frac{\partial}{\partial x}\left(\mathcal{D}_{\pm}\exp(\pm\bar{\varphi})\frac{\partial \mathrm{f}_1^{\pm}}{\partial x}\right)+\frac{\partial}{\partial y}\left(\mathcal{D}_{\pm}\exp(\pm\bar{\varphi})\frac{\partial \mathrm{f}_1^{\pm}}{\partial y}\right)$$

$$=\pm\boldsymbol{e}^1\mathcal{D}_{\pm}\cdot\exp(\pm\bar{\varphi})\tfrac{\partial\bar{\varphi}}{\partial y}\boldsymbol{e}^2, \tag{3.8}$$

$$\frac{\partial \mathrm{f}_1^{\pm}}{\partial y}=-\boldsymbol{e}^1\cdot\boldsymbol{n}=-\boldsymbol{e}^1\cdot\boldsymbol{e}^2 \quad \text{at } y=H$$

and

$$\frac{\partial}{\partial x}\left(\mathcal{D}_{\pm}\exp(\pm\bar{\varphi})\frac{\partial \mathrm{f}_2^{\pm}}{\partial x}\right)+\frac{\partial}{\partial y}\left(\mathcal{D}_{\pm}\exp(\pm\bar{\varphi})\frac{\partial \mathrm{f}_2^{\pm}}{\partial y}\right)$$

$$=\pm\mathcal{D}_{\pm}\boldsymbol{e}^2\cdot\exp(\pm\bar{\varphi})\tfrac{\partial\bar{\varphi}}{\partial y}\boldsymbol{e}^2, \tag{3.9}$$

$$\frac{\partial \mathrm{f}_2^{\pm}}{\partial y}=-\boldsymbol{e}^2\cdot\boldsymbol{n}=-\boldsymbol{e}^2\cdot\boldsymbol{e}^2=-1 \quad \text{at } y=H.$$

Likewise, the notation κ_I adopted for the axial conductivities, in what follows we denote $\{g_I, h_I^{\pm}\}$ the component $j=1$ of $\{g_I^{\mathrm{j}}, h_I^{\pm j}\}(I=\mathrm{p},\mathrm{c},\mathrm{e})$ in (2.9)–(2.11). Thus, in terms of $\{\kappa_{\mathrm{p}}, g_{\mathrm{p}}, h_{\mathrm{p}}^{\pm}\}$ the closure problem (2.9) can be rephrased as

$$\mu_{\mathrm{f}}\frac{\partial^2\kappa_{\mathrm{p}}}{\partial y^2}-\frac{\partial g_{\mathrm{p}}}{\partial x}-A\frac{\partial h_{\mathrm{p}}^{+}}{\partial x}-B\frac{\partial h_{\mathrm{p}}^{-}}{\partial x}=-1,$$

$$-\frac{\partial g_{\mathrm{p}}}{\partial y}-A\frac{\partial h_{\mathrm{p}}^{+}}{\partial y}-B\frac{\partial h_{\mathrm{p}}^{-}}{\partial y}=0, \quad \frac{\partial\kappa_{\mathrm{p}}}{\partial x}=0,$$

$$\frac{\partial}{\partial x}\left(\mathcal{D}_{\pm}\exp(\mp\bar{\varphi})\frac{\partial h_{\mathrm{p}}^{\pm}}{\partial x}\right)+\frac{\partial}{\partial y}\left(\mathcal{D}_{\pm}\exp(\mp\bar{\varphi})\frac{\partial h_{\mathrm{p}}^{\pm}}{\partial y}\right) \tag{3.10}$$

$$=\mp\kappa_{\mathrm{p}}\boldsymbol{e}^1\cdot\exp(\mp\bar{\varphi})\tfrac{\partial\bar{\varphi}}{\partial y}\boldsymbol{e}^2,$$

$$\kappa_{\mathrm{p}}=0, \quad \frac{\partial h_{\mathrm{p}}^{\pm}}{\partial y}=0 \quad \text{at } y=H,$$

whereas the axial components of the chemico-osmotic and electro-osmotic permeabilities are governed by

$$
\begin{aligned}
&\mu_f \frac{\partial^2 \kappa_c}{\partial y^2} - \frac{\partial g_c}{\partial x} - A\frac{\partial h_c^+}{\partial x} - B\frac{\partial h_c^-}{\partial x} = -F^1,\\
&-\frac{\partial g_c}{\partial y} - A\frac{\partial h_c^+}{\partial y} - B\frac{\partial h_c^-}{\partial y} = -F^2, \qquad \frac{\partial \kappa_c}{\partial x} = 0,\\
&\frac{\partial}{\partial x}\left(\mathcal{D}_\pm \exp(\mp\bar{\varphi})\frac{\partial h_c^\pm}{\partial x}\right) + \frac{\partial}{\partial y}\left(\mathcal{D}_\pm \exp(\mp\bar{\varphi})\frac{\partial h_c^\pm}{\partial y}\right) = \mp\kappa_c \boldsymbol{e}^1 \cdot \exp(\mp\bar{\varphi})\frac{\partial \bar{\varphi}}{\partial y}\boldsymbol{e}^2,\\
&\kappa_c = 0, \quad \frac{\partial h_c^\pm}{\partial y} = 0 \quad \text{at } y = H
\end{aligned}
\tag{3.11}
$$

and

$$
\begin{aligned}
&\mu_f \frac{\partial^2 \kappa_e}{\partial y^2} - \frac{\partial g_e}{\partial x} - A\frac{\partial h_e^+}{\partial x} - B\frac{\partial h_e^-}{\partial x} = -G^1,\\
&-\frac{\partial g_e}{\partial y} - A\frac{\partial h_e^+}{\partial y} - B\frac{\partial h_e^-}{\partial y} = -G^2, \qquad \frac{\partial \kappa_e}{\partial x} = 0,\\
&\frac{\partial}{\partial x}\left(\mathcal{D}_\pm \exp(\mp\bar{\varphi})\frac{\partial h_e^\pm}{\partial x}\right) + \frac{\partial}{\partial y}\left(\mathcal{D}_\pm \exp(\mp\bar{\varphi})\frac{\partial h_e^\pm}{\partial y}\right)\\
&\quad = \mp\kappa_e \boldsymbol{e}^1 \cdot \exp(\mp\bar{\varphi})\frac{\partial \bar{\varphi}}{\partial y}\boldsymbol{e}^2,\\
&\kappa_e = 0, \quad \frac{\partial h_e^\pm}{\partial y} = 0 \quad \text{at } y = H,
\end{aligned}
\tag{3.12}
$$

where from (2.12) the scalars $\{F^1, F^2, G^1, G^2\}$ are given as

$$
\begin{aligned}
F^1 &= RT\left(2(\cosh\bar{\varphi} - 1) + (\exp(-\bar{\varphi}) - 1)\frac{\partial f_1^+}{\partial x} + (\exp(+\bar{\varphi}) - 1)\frac{\partial f_1^-}{\partial x}\right),\\
F^2 &= RT\left((\exp(-\bar{\varphi}) - 1)\frac{\partial f_2^+}{\partial x} + (\exp(+\bar{\varphi}) - 1)\frac{\partial f_2^-}{\partial x}\right),\\
G^1 &= RTc_b\left(-2\sinh\bar{\varphi} + (\exp(-\bar{\varphi}) - 1)\frac{\partial f_1^+}{\partial x} - (\exp(\bar{\varphi}) - 1)\frac{\partial f_1^-}{\partial x}\right),\\
G^2 &= RTc_b\left((\exp(-\bar{\varphi}) - 1)\frac{\partial f_2^+}{\partial x} - (\exp(\bar{\varphi}) - 1)\frac{\partial f_2^-}{\partial x}\right).
\end{aligned}
\tag{3.13}
$$

The closure problems (2.7) for $\{\boldsymbol{\xi}, \boldsymbol{\zeta}\}$ are classical mechanical problems which also appear in the homogenization of Biot's theory of poroelasticity (Auriault and Sanchez-Palencia, 1977; Auriault, 1990; Terada *et al.*, 1998; Lydzba and Shao, 2000). For parallel particles, the traction boundary conditions only act in the direction normal to the clay surface and therefore

the only relevant component of $\{\boldsymbol{\xi}, \boldsymbol{\zeta}\mathbf{u}_\pi\}$ is the one normal to the clay surface denoted herein by $\{\xi, \zeta u_\pi\}$. Thus, invoking the periodicity, dropping the derivatives with respect to x and denoting $c_s = \lambda_s + 2\mu_s$ the scalar elastic, modulus of the isotropic particles, the one-dimensional versions of (2.7) and 2.5(b) read as

$$\left|\begin{array}{l} c_s \dfrac{d^2\zeta}{dy^2} = 0 \\ c_s \dfrac{d\zeta}{dy} = -1 \quad \text{at } y = \pm H, \end{array}\right. \quad \left|\begin{array}{l} c_s \dfrac{d^2\xi}{dy^2} = 0 \\ \dfrac{d\xi}{dy} = -1 \quad \text{at } y = \pm H, \end{array}\right. \quad \left\{\begin{array}{l} c_s \dfrac{d^2 u_\pi}{dy^2} = 0 \\ c_s \dfrac{du_\pi}{dy} = -\Pi_d \quad \text{at } y = \pm H, \end{array}\right. \tag{3.14}$$

Finally, denoting $\{\Pi, \Pi_S, C_s, \alpha\}$ the components of the coefficients $\{\boldsymbol{\Pi}, \boldsymbol{\Pi}_S, \boldsymbol{C}_s, \boldsymbol{\alpha}\}$ normal to the clay surface and $\{K_I, D^i_\pm, v_\pm\}$, $(I = P, C, E$ and i = p, c, e) the axial component of $\{\boldsymbol{K_I}, \boldsymbol{D}^{\boldsymbol{I}}_\pm, \mathbf{v}_\pm\}$, from (2.6) the representations of these reduced quantities and of the compressibilities $\{\beta, \gamma_\pi\}$ are given by

$$\begin{aligned} &\Pi = \langle \Pi_d \rangle + n_s \Pi_S, \quad \Pi_S = -c_s \left\langle \frac{du_\pi}{dy} \right\rangle^s, \quad C_s = c_s \left\langle \left(1 + \frac{\partial \xi}{\partial y}\right) \right\rangle, \quad \alpha = n_f - \left\langle \frac{\partial \xi}{\partial y} \right\rangle, \\ &D^I_\pm = \mathcal{D}_\pm \left\langle \exp(\pm\bar{\varphi}) \left(1 + \frac{\partial f^\pm_1}{\partial x} + c_b \frac{\partial h^\pm_I}{\partial x}\right) \right\rangle^f \boldsymbol{I} = c, e, \quad D^p_\pm = \mathcal{D}_\pm \left\langle \exp(\pm\bar{\varphi}) \frac{\partial h^\pm_p}{\partial x} \right\rangle^f, \\ &\beta = \left\langle \frac{\partial \zeta}{dy} \right\rangle, \quad \gamma_\pi = \left\langle \frac{du_\pi}{dy} \right\rangle, \quad G_\pm v_\pm = \langle v \exp(\mp\bar{\varphi}) \rangle, \quad K_{\boldsymbol{I}} = \langle \kappa_i \rangle, \quad I = P, C, E \quad \text{i} = \text{p, c, e.} \end{aligned} \tag{3.15}$$

3.2. FURTHER MANIPULATIONS IN THE REDUCED CLOSURE PROBLEMS

We now proceed by establishing direct correlations between the magnitude of the effective electro-chemo-mechanical coefficients and the local distribution of the e.d.l. potential $\bar{\varphi} = \bar{\varphi}(y)$. This is accomplished by further manipulating the aforementioned reduced closure problems. In the subsequent development, such correlations are exploited to compute the constitutive dependence of the effective parameters on concentration c_b and particle separation H.

3.2.1. *Poroelastic Coefficients*

We begin by analyzing the mechanical parameters $\{\alpha, \xi, \zeta, \beta\}$ which also appear in the classical micromechanical derivation of poroelasticity (Auriault, 1990; Terada *et al.*, 1998; Lydzba and Shao, 2000). From (3.14)(a)(b) we obtain $\partial\xi/\partial y = c_s \partial\zeta/\partial y = -1$ which yields after averaging $c_s\langle d\zeta/dy\rangle = \langle d\xi/dy\rangle = -n_s$. Using this result in (3.15) we get $\alpha = n_f + n_s = 1$, $\beta = -n_s/c_s$ and $C_s = 0$. Hence, as expected for a parallel particle arrangement, typical of Low's experiment (Low, 1987), the component of the contact elastic stress σ_e normal to the clay surface vanishes and the compression load is solely sustained by the electro-chemical component Π. In addition, the

mechanical compressibility β is nothing but the inverse of the microscopic bulk modulus of the particles. Finally, one may note that as the transversal elastic modulus C_s vanishes, the closure relation for α is consistent with its classical representation $\alpha = 1 - C_s/c_s = 1$ proposed by Biot and Willis (1957).

3.2.2. *Local Electrostatics*

Now consider the local distributions in the y-direction of the e.d.l. potential $\bar{\varphi}$ and normal electric field E. The solution of the one-dimensional Poisson–Boltzmann problem (3.7) can be represented in terms of the electric potential in the line of symmetry $\bar{\varphi}(y=0) = \bar{\varphi}_0$. By multiplying (3.7) by $\mathrm{d}\bar{\varphi}/\mathrm{d}y$ and integrating from 0 to y we obtain

$$\frac{\tilde{\varepsilon}\tilde{\varepsilon}_0}{2}\left(\frac{\mathrm{d}\bar{\varphi}}{\mathrm{d}y}\right)^2 = \frac{2F^2 c_\mathrm{b}}{RT}\int_{\bar{\varphi}_0}^{\bar{\varphi}} \sinh\bar{\varphi}\,\mathrm{d}\bar{\varphi} = \frac{2F^2 c_\mathrm{b}}{RT}(\cosh\bar{\varphi} - \cosh\bar{\varphi}_0), \tag{3.16}$$

which yields

$$E = -\frac{RT}{F}\frac{\mathrm{d}\bar{\varphi}}{\mathrm{d}y} = 2\sqrt{\frac{RTc_b}{\tilde{\varepsilon}\tilde{\varepsilon}_0}(\cosh\bar{\varphi} - \cosh\bar{\varphi}_0)},$$
$$\bar{\varphi} = \bar{\varphi}_0 - 2F\int_0^y \sqrt{\frac{c_b}{\tilde{\varepsilon}\tilde{\varepsilon}_0 RT}(\cosh\bar{\varphi} - \cosh\bar{\varphi}_0)}\,\mathrm{d}y. \tag{3.17}$$

The above result leads to a non-linear equation for $\bar{\varphi}$ which can be solved adopting a numerical iterative integration scheme (see further, Section 4).

In what follows we proceed by further manipulating the subsequent closure problems. Begin by noting that under the orthogonality condition between $\boldsymbol{e}^1$ and $\boldsymbol{e}^2$, the r.h.s. of (3.8) vanishes. Together with the periodicity conditions this leads to a homogeneous Neumann problem whose solution is $f_1^{\pm} = f_1^{\pm}(t)$ within each cell. By the same arguments, on the right hand side of the third equations in (3.10)–(3.12) vanish. Together with the periodicity this also yields $h_i^{\pm} = h_i^{\pm}(t)$ (i = p, c, e). Finally, again using the periodicity, from (3.9) we have, $f_2^{\pm} = f_2^{\pm}(y, t)$.

3.2.3. *Hydraulic Conductivity*

Using the above simplifications, the problem (3.10) left for $\{\kappa_\mathrm{p}, g_\mathrm{p}\}$ reduces to

$$\mu_\mathrm{f}\frac{\partial^2\kappa_\mathrm{p}}{\partial y^2} - \frac{\partial g_\mathrm{p}}{\partial x} = -1,$$
$$\frac{\partial g_\mathrm{p}}{\partial y} = 0, \qquad \frac{\partial \kappa_\mathrm{p}}{\partial x} = 0,$$
$$\kappa_\mathrm{p} = 0, \quad \text{at } y = \pm H$$

in which together with the periodicity implies g_p = cte and the classical parabolic profile $\kappa_p = \kappa_p(y)$, satisfying

$$\mu_f \frac{d^2\kappa_p}{dy^2} = -1. \tag{3.18}$$

Denoting 2δ the thickness of each clay particle, in the stratified arrangement, the porosity is given by $n_f = H/(\delta + H)$. Defining the hydraulic conductivity K_P by the transversal averaging of the local parabolic velocity profile κ_p, we have

$$K_P = \langle \kappa_p \rangle = \frac{n_f}{H} \int_0^H \kappa_p dy = \frac{n_f H^2}{3\mu f} = \frac{H^3}{3(\delta + H)\mu_f}.$$

The above result shows that for parallel particles K_P remains a purely geometric quantity only influenced by fluid viscosity and particle distance and thickness. The reader shall be aware that this result is restricted to parallel particles. Local variations in $h_p^{\pm}$ and $\bar{\varphi}$ in non-parallel particle arrangements entail a more general constitutive dependence of K_P on the e.d.l. properties and salinity.

3.2.4. *Electro-Osmotic Permeability*

Using the fact that $f_1^{\pm}$ and $f_2^{\pm}$ are independent of x in (3.13) we obtain $G^2 = 0$ and $G^1 = -2RTc_b \sinh \bar{\varphi}$. Thus, from (3.12), in a similar fashion to K_P, the axial component of the electro-osmotic permeability, K_E is the transversal averaging of the velocity profile satisfying the local problem

$$\mu_f \frac{d^2\kappa_e}{dy^2} = 2RTc_b \sinh \bar{\varphi}.$$

Hence, unlike K_P, the magnitude of K_E is strongly dictated by the local distribution $\bar{\varphi} = \bar{\varphi}(y)$. Combining the above result with the Poisson–Boltzmann problem (3.7) gives

$$\mu_f \frac{d^2\kappa_e}{dy^2} = \frac{\tilde{\varepsilon}\tilde{\varepsilon}_0 R^2 T^2}{F^2} \frac{d^2\bar{\varphi}}{dy^2}. \tag{3.19}$$

After integration, making use of the symmetry at $y = 0$ and the no-slip condition at $y = H$ implies

$$\mu_f \frac{d\kappa_e}{dy}(y) = \frac{\tilde{\varepsilon}\tilde{\varepsilon}_0 R^2 T^2}{F^2} \frac{d\bar{\varphi}}{dy}(y), \qquad \kappa_e(y) = \frac{\tilde{\varepsilon}\tilde{\varepsilon}_0 R^2 T^2}{\mu_f F^2} (\bar{\varphi}(y) - \bar{\varphi}(H)).$$

Hence, defining the dimensionless zeta potential $\bar{\zeta} = \bar{\varphi}(H)$, after averaging we obtain

$$K_{\mathrm{E}} = \frac{n_{\mathrm{f}}}{H}\int_0^H \kappa_{\mathrm{e}}\mathrm{d}y = \frac{n_{\mathrm{f}}\tilde{\varepsilon}\tilde{\varepsilon}_0 R^2T^2}{F^2 H\mu_{\mathrm{f}}}\int_0^H (\bar{\varphi}(y)-\bar{\varphi}(H))\mathrm{d}y$$
$$= \frac{n_{\mathrm{f}}\tilde{\varepsilon}\tilde{\varepsilon}_0 R^2T^2}{\mu_{\mathrm{f}}F^2}\left(\langle\bar{\varphi}\rangle^{\mathrm{f}} - \bar{\zeta}\right). \tag{3.20}$$

When the thickness of the e.d.l. is small compared to the interlayer spacing H, the Helmholtz–Smoluchowski model can be recovered from (3.20). Under this assumption the first term involving $\langle\bar{\varphi}\rangle^{\mathrm{f}}$ is small compared to the magnitude of the $\bar{\zeta}$-potential. This approximation yields

$$K_{\mathrm{E}} = -\frac{n_{\mathrm{f}}\tilde{\varepsilon}\tilde{\varepsilon}_0\zeta RT}{F\mu_{\mathrm{f}}}, \tag{3.21}$$

where $\zeta \equiv RT\bar{\zeta}/F$. The above result which is nothing but the Smoluchowski's formula for thin e.d.l.s (Hunter, 1981; Coelho *et al.*, 1996; Shang, 1997). We remark that the appearance of the extra factor RT/F is a consequence of adopting $\nabla\bar{\psi}_{\mathrm{b}}$ as a driving force in (3.2) (rather than $\nabla\bar{\psi}_{\mathrm{b}}$).

From (3.20) one may extract relevant information on the sources of electro-osmosis. The Smoluchowski term is a primary component which relates the electro-osmotic permeability with the ζ-potential at the surface. This term dominates the magnitude of K_{E} for large particle distances ($H \gg \ell_{\mathrm{D}}$). The secondary contribution involving $\langle\bar{\varphi}\rangle^{\mathrm{f}}$ arises from the overlapping between the e.d.l.s and becomes relevant when $H = \mathcal{O}(\ell_{\mathrm{D}})$. This component acts to decrease the electro-osmotic permeability and has been incorporated in Smolucbowski's formula by means of a correction factor (see Hunter, 1981; Szymczyk *et al.*, 1999).

3.2.5. *Chemico-osmotic Permeability*

Under the same previous assumptions, from (3.13) we have $F^2 = 0$ and $F^1 = 2RT(\cosh\bar{\varphi} - 1)$. This implies that the axial component of the chemico-osmotic permeability is the averaging of the characteristic function κ_{c} satisfying

$$\mu_{\mathrm{f}}\frac{\mathrm{d}^2\kappa_{\mathrm{c}}}{\mathrm{d}y^2} = -2RT(\cosh\bar{\varphi} - 1). \tag{3.22}$$

Likewise the Smoluchowski's asymptotic regime governing the electro-osmotic permeability for large particle distances, we can obtain the limit model of thin e.d.l.s for the chemico-osmotic permeability. To this end we use instead a coordinate $y' = y - H$ such at $y' = 0$ at the particle surface. In addition, under the assumption $\ell_{\mathrm{D}} << H$, electrical effects are absent away from the particle surface. This enforces the conditions $\bar{\varphi} = \mathrm{d}\bar{\varphi}/\mathrm{d}y' = 0$

as $y' \to \infty$. Thus, integrating (3.22) from y' to ∞ and using the thin e.d.l. assumption we get

$$\mu_f \frac{d\kappa_c}{dy'} = 2RT \int_{y'}^{\infty} (\cosh \bar{\varphi} - 1) dy' \tag{3.23}$$

where the right-hand side can be rewritten using the identity

$$2(\cosh \bar{\varphi} - 1) = 4 \sinh^2 \frac{\bar{\varphi}}{2} = \frac{16 \tanh^2 \bar{\varphi}/4}{\left(1 - \tanh^2 \bar{\varphi}/4\right)^2}. \tag{3.24}$$

Using Poisson–Boltzmann one can relate $\tanh(\bar{\varphi}/4)$ to the dimensionless zeta potential $\bar{\zeta} \equiv \bar{\varphi}(H)$. To this end we multiply (3.7) by 2 $d\bar{\varphi}/dy'$ to obtain

$$\frac{d}{dy'} \left(\frac{d\bar{\varphi}}{dy'} \right)^2 = \frac{2}{\ell_D^2} \frac{d}{dy'} \cosh \bar{\varphi}. \tag{3.25}$$

Integrating (3.25) from ∞ to y' and using (3.24) gives

$$\left(\frac{d\bar{\varphi}}{dy'} \right)^2 = \frac{2}{\ell_D^2} (\cosh \bar{\varphi} - 1) = \frac{4}{\ell_D^2} \sinh^2 \left(\frac{\bar{\varphi}}{2} \right).$$

Hence we have

$$\frac{d\bar{\varphi}}{dy'} = -\frac{2}{\ell_D} \sinh \left(\frac{\bar{\varphi}}{2} \right) \quad \to \quad \frac{d\bar{\varphi}}{\sinh(\bar{\varphi}/2)} = -\frac{2}{\ell_D} dy'. \tag{3.26}$$

To integrate the above result we adopt the following change of variables

$$w = \tanh \left(\frac{\bar{\varphi}}{4} \right) \qquad dw = \tfrac{1}{4}(1 - w^2) d\bar{\varphi}, \qquad \sinh \left(\frac{\bar{\varphi}}{2} \right) = \frac{2w}{1 - w^2}. \tag{3.27}$$

Using (3.27) in (3.26)(b) we get

$$\frac{dw}{w} = -\frac{dy'}{\ell_D} \tag{3.28}$$

which gives after integrating from 0 to y'

$$\ln \left[\frac{\tanh(\bar{\varphi}/4)}{\tanh(\bar{\zeta}/4)} \right] = -\frac{y'}{\ell_D}.$$

Whence

$$\tanh \left(\frac{\bar{\varphi}}{4} \right) = \tanh \left(\frac{\bar{\zeta}}{4} \right) \exp \left(-\frac{y'}{\ell_D} \right).$$

Denoting $A = \tanh(\bar{\zeta}/4)$, using the above result in (3.24) we get

$$2(\cosh\bar{\varphi} - 1) = \frac{16A^2\exp(-2y'/\ell_D)}{[1 - A^2\exp(-2y'/\ell_D)]^2}. \tag{3.29}$$

Denoting $u = A^2\exp(-2y'/\ell_D)$ with $du = -(2u/\ell_D)dy'$, integrating (3.29) we obtain

$$2\int_{y'}^{\infty}(\cosh\bar{\varphi} - 1)dy' = 8\ell_D\int_0^u \frac{du}{(1-u^2)} = \frac{8\ell_D u}{1-u}.$$

Using the above result in (3.23) yields

$$\mu_f\frac{d\kappa_c}{dy'} = \frac{8RT\ell_D A^2\exp(-2y'/\ell_D)}{1 - A^2\exp(-2y'/\ell_D)}.$$

in which after integrating from 0 to y' and using the nonslip condition at the wall yields

$$\begin{aligned}\kappa_c(y') &= \frac{8RT\ell_D}{\mu_f}\int_0^{y'}\frac{A^2\exp(-2y'/\ell_D)}{1 - A^2\exp(-2y'/\ell_D)}dy' = -\frac{4RT\ell_D^2}{\mu_f}\int_{A^2}^{u}\frac{du}{1-u}\\ &= \frac{4RT\ell_D^2}{\mu_f}[\ln(1-u)]_{A^2}^{u}\\ &= \frac{4RT\ell_D^2}{\mu_f}\ln\left[\frac{1 - \tanh^2(\bar{\zeta}/4)\exp(-2y'/\ell_D)}{1 - \tanh^2(\bar{\zeta}/4)}\right].\end{aligned}$$

In a similar fashion to K_E, the above result shows the magnitude of K_C given by the sum of two contributions: one solely dictated by the $\bar{\zeta}$-potential, playing a similar role of the Smoluchowski's component of K_E, which dominates the behavior of K_C for $H >> \ell_D$, and a secondary e.d.l component, strongly dependent on the Debye's length, which becomes pronounced when $H = \mathcal{O}(\ell_D)$. In the asymptotic regime of thin e.d.l.s the primary component of κ_c is independent of y' and therefore equal to its averaged value K_C. We then have the asymptotic result

$$K_C = -\frac{4RT\ell_D^2}{\mu_f}\ln\left(1 - \tanh^2\left(\frac{\bar{\zeta}}{4}\right)\right) = \frac{8RT\ell_D^2}{\mu_f}\ln\left(\cosh\left(\frac{\bar{\zeta}}{4}\right)\right) \quad \text{for } \ell_D \ll H. \tag{3.30}$$

The above formula is consistent with the results obtained by Derjaguin *et al.* (1961) and Prieve *et al.* (1984) relating fluid velocity with the $\bar{\zeta}$-potential considering flow near an infinite surface charged particle with thin e.d.l.s.

3.2.6. *Local Velocity Profile*

Taking the second derivative with respect to y in the decomposition (3.2) for the axial velocity and using the reduced closure problems (3.18), (3.22) and (3.19) for $\{\boldsymbol{\kappa}_{\mathrm{p}}, \boldsymbol{\kappa}_{\mathrm{c}}, \boldsymbol{\kappa}_{\mathrm{e}}\}$ we obtain

$$\mu_{\mathrm{f}} \frac{\mathrm{d}^2 v}{\mathrm{d}y^2} = \frac{\mathrm{d}p_{\mathrm{b}}}{\mathrm{d}x} + 2RT(\cosh\bar{\varphi} - 1) \quad \frac{\mathrm{d}c_{\mathrm{b}}}{\mathrm{d}x} - \frac{\tilde{\varepsilon}\tilde{\varepsilon}_0 R^2 T^2}{F^2} \frac{\mathrm{d}^2\bar{\varphi}}{\mathrm{d}y^2} \frac{\mathrm{d}\bar{\psi}_{\mathrm{b}}}{\mathrm{d}x}.$$

The above modified Stokes problem shows the local axial velocity as a superposition of characteristic hydraulic, chemico-osmotic and electro-osmotic profiles with the corresponding driving forces appearing on the right-hand side.

3.2.7. *Diffusion Coefficients*

Using the simplifications for $\mathrm{f}_1^{\pm}$ and $h_I^{\pm}(I = \mathrm{p}, \mathrm{c}, \mathrm{e})$ in (3.15), the representations of the axial diffusion coefficients reduce to

$$D_{\pm}^{\mathrm{p}} = 0 \quad \text{and} \quad D_{\pm}^{\mathrm{c}} = D_{\pm}^{\mathrm{e}} = D_{\pm} = \mathcal{D}_{\pm}\langle \exp(\mp\bar{\varphi})\rangle^{\mathrm{f}}. \tag{3.31}$$

Using the above results and the representation in (3.15) for $v_{\pm}$ in (2.2) and (2.3) the axial movement of the ions is governed by the one-dimensional Nernst–Planck equation

$$\frac{\partial}{\partial t}\left(n_{\mathrm{f}}\langle \exp(\mp\bar{\varphi})\rangle^{\mathrm{f}} c_{\mathrm{b}}\right) + \frac{\partial}{\partial x}\left(\langle \exp(\mp\bar{\varphi}) v\rangle c_{\mathrm{b}}\right)$$
$$= \frac{\partial}{\partial x}\left(n_{\mathrm{f}}\mathcal{D}_{\pm} \exp(\mp\bar{\varphi}) \left(\frac{\partial c_{\mathrm{b}}}{\partial x} \pm c_{\mathrm{b}} \frac{\partial \bar{\psi}_{\mathrm{b}}}{\partial x}\right)\right).$$

3.2.8. *Disjoining and Deviatoric Stresses*

Using (3.16) in (3.4) the microscopic disjoining pressure can be represented as

$$\Pi_{\mathrm{d}} = 2RTc_{\mathrm{b}}(\cosh\bar{\varphi} - 1) - \frac{\tilde{\varepsilon}\tilde{\varepsilon}_0 R^2 T^2}{2F^2}\left(\frac{\mathrm{d}\bar{\varphi}}{\mathrm{d}y}\right)^2 = 2RTc_{\mathrm{b}}(\cosh\bar{\varphi}_0 - 1). \tag{3.32}$$

The above result is consistent with the e.d.l. theory and shows Π_{d} constant in the micro-pore space, given only in terms of the potential $\bar{\varphi}_0$ in the middle of the interlayer spacing. Further, from (3.6) and (3.17) (a), the deviatoric component of the stress tensor in the fluid is represented as $\boldsymbol{S} = S_{11}\boldsymbol{e}^1 \otimes \boldsymbol{e}^1 + S_{22}\boldsymbol{e}^2 \otimes \boldsymbol{e}^2$ with

$$S_{11} = -S_{22} = \frac{\tilde{\varepsilon}\tilde{\varepsilon}_0 E^2}{2} = 2RTc_{\mathrm{b}}(\cosh\bar{\varphi}_0 - \cosh\bar{\varphi}).$$

Note that, as the deviatoric stresses are purely related to the Maxwell stress tensor, in the line of symmetry $y=0$ where E and $\boldsymbol{\tau_M}$ vanish we also have $S_{11}=S_{22}=0$.

In addition to the excess in the normal pressure relative to the bulk phase pressure, quantified by the disjoining pressure, ($\Pi_d = p_n - p_b$), the appearance of a equilibrium deviatoric stress in the liquid gives rise to the excess in the tangential pressure component relative to both normal and bulk phase pressures. The constitutive relations for these quantities follow from (3.5), (3.16) and (3.32) and are given by

$$p_t - p_n = \tilde{\varepsilon}\tilde{\varepsilon}_0 E^2 = \frac{\tilde{\varepsilon}\tilde{\varepsilon}_0 R^2 T^2}{F^2}\left(\frac{d\bar{\varphi}}{dy}\right)^2 = 4RTc_b(\cosh\bar{\varphi} - \cosh\bar{\varphi}_0), \tag{3.33}$$

$$p_t - p_b = \Pi_d + \tilde{\varepsilon}\tilde{\varepsilon}_0 E^2 = 2RTc_b(2\cosh\bar{\varphi} - \cosh\bar{\varphi}_0 - 1). \tag{3.34}$$

3.2.9. *Swelling Pressure*

To compute the macroscopic electro-chemical components Π and Π_S acting normal to the particle surface we begin by combining the solution of (3.14)(c) with the representation for Π_S in (3.15) which gives $\Pi_S = -c_s\langle du_\pi/dy\rangle^s = \langle\Pi_d\rangle^s$. Recalling from (3.32) that Π_d does not vary with y, we have $\Pi_S = \Pi_d$. Moreover combining this result with (3.15) we obtain

$$\Pi = \langle\Pi_d\rangle + n_s\Pi_S = n_f\Pi_d + n_s\Pi_S = \Pi_S(n_f + n_s) = \Pi_S.$$

The component Π_S acting normal to the clay surface has been commonly referred to as the swelling pressure in the sense of Low (1987). In the parallel particle arrangement Π_s has been identified with the pressure that must be applied to the clay to keep the layers from moving apart. The equality $\Pi_d = \Pi_s$ reproduces Derjaguin's conjecture (Derjaguin *et al.*, 1987) which states that the swelling pressure is nothing but the averaged disjoining pressure. We remark that the validity of this result is restricted to microgeometries of parallel particles.

3.2.10. *Surface and Liquid Tensions*

Following the generalized Baker's formula for thin liquid films, the liquid tension γ_{fs} and the surface tension σ_{fs} are defined by the transversal averages of the excess quantities given in (3.33) and (3.34) (see, e.g., Toshev and Ivanov, 1975; Derjaguin and Churaev, 1978; Babak, 1998). We then have

$$\gamma_{fs} \equiv -\int_{-H}^{H}(p_t - p_n)dy = -2\int_0^H (p_t - p_n)dy$$
$$= -8RTc_b\int_0^H(\cosh\bar{\varphi} - \cosh\bar{\varphi}_0)dy,$$

$$\sigma_{\rm fs} \equiv -\int_0^H (p_{\rm t} - p_{\rm b}){\rm d}h = -\int_0^H (\tilde{\varepsilon}\tilde{\varepsilon}_0 E^2 + \Pi_{\rm d})$$
$$= -2RTc_{\rm b}\int_0^H (2\cosh\bar{\varphi} - \cosh\bar{\varphi}_0 - 1){\rm d}y.$$

Unlike the swelling pressure, $\gamma_{\rm fs}$ and $\sigma_{\rm fs}$ are not effective quantities as both act compressing the fluid tangentially to the solid surface and consequently do not induce any expansion or shrinking in the clay lattice. The relation between these quantities and the disjoining pressure is given by

$$\gamma_{\rm fs} \equiv -2\int_0^H (p_{\rm t} - p_{\rm n}){\rm d}y = -2\int_0^H (p_{\rm t} - p_{\rm b}){\rm d}y + 2\int_0^H (p_{\rm n} - p_{\rm b}){\rm d}y$$
$$= 2\sigma_{\rm fs} + 2\int_0^H \Pi_{\rm d}{\rm d}y = 2\sigma_{\rm fs} + 2\Pi_{\rm d}H,$$

where we have used the independence of $\Pi_{\rm d}$ with y. The above result is consistent with Toshev and Ivanov (1975) and Babak (1998).

3.2.11. *Electro-Chemical Compressibility*

Using the relations $c_{\rm s}{\rm d}u_\pi/{\rm d}y = -\Pi_{\rm d}$ and (3.32) in the representation of the electro-chemical compressibility γ_π in (3.15) we obtain

$$\gamma_\pi = n_{\rm s}\left\langle \frac{{\rm d}u_\pi}{{\rm d}y}\right\rangle^{\rm s} = -\frac{n_{\rm s}\Pi_{\rm d}}{c_{\rm s}} = -\frac{2RTn_{\rm s}c_{\rm b}}{c_{\rm s}}(\cosh\bar{\varphi}_0 - 1), \tag{3.35}$$

which shows that γ_π quantifies the deformation of the solid phase induced by the disjoining pressure owing to particle compressibility.

Finally, recalling the result $\beta = -n_{\rm s}/c_{\rm s}$ (Section 3.2.1), for microscopically incompressible particles. we have $c_{\rm s} \to \infty$ which implies $\beta = \gamma_\pi = 0$.

3.2.12. *Onsager's Coefficients*

We now consider the microscopic reduced representations of the Onsager's parameters. Begin by invoking definitions in (2.14) for the overall and excess quantities and denote $\{D_*^I, \Delta_*^I\}$ the axial components of $\{\boldsymbol{D}_*^I, \boldsymbol{\Delta}_*^I\}(I =$ p, c, e). Using (3.31) we have the representations

$$D_*^{\rm p} = 0, \quad D_*^{\rm c} = D_*^{\rm e} = D_* = \mathcal{D}_+\langle\exp(-\bar{\varphi})\rangle^{\rm f} + \mathcal{D}_-\langle\exp(-\bar{\varphi})\rangle^{\rm f}, \tag{3.36}$$

and

$$\Delta_*^{\rm p} = 0, \quad \Delta_*^{\rm c} = \Delta_*^{\rm e} = \Delta_* = \mathcal{D}_+\langle\exp(-\bar{\varphi})\rangle^{\rm f} + \mathcal{D}_-\langle\exp(-\bar{\varphi})\rangle^{\rm f}.$$

We adopt the notation $L_{\rm IJ}$ (without boldface) to represent the scalar axial component of the Onsager's coefficient obtained by replacing $\{\boldsymbol{\kappa}_I, \boldsymbol{D}_*^I, \boldsymbol{\Delta}_*^I\}$(I = p, c, e) by their corresponding axial components $\{\kappa_I, D_*^I, \Delta_*^I\}$ in

(2.21). Denoting $\{v_D, J_c, I_e\}$ the axial components of $\{\mathbf{v}_D, \boldsymbol{J}_c, \boldsymbol{I}_e\}$, the one-dimensional version of (2.20) reads

$$\begin{aligned} v_D &= -L_{PP}\frac{dp_b}{dx} - L_{PC}\frac{RT}{c_b}\frac{dc_b}{dx} - L_{PE}\frac{d\psi_b}{dx}, \\ J_c &= -L_{CP}\frac{dp_b}{dx} - L_{CC}\frac{RT}{c_b}\frac{dc_b}{dx} - L_{CE}\frac{d\psi_b}{dx}, \\ I_e &= -L_{EP}\frac{dp_b}{dx} - L_{EC}\frac{RT}{c_b}\frac{dc_b}{\partial x} - L_{EE}\frac{d\psi_b}{dx} \end{aligned} \tag{3.37}$$

with axial components of $\boldsymbol{L}_{IJ}$ in (2.21) given by

$$\begin{aligned} &L_{PP} = K_P, \quad L_{PC} = \frac{c_b K_C}{RT}, \quad L_{PE} = \frac{F K_E}{RT}, \\ &L_{CP} = 2c_b\langle\kappa_p(\cosh\bar{\varphi} - 1)\rangle, \quad L_{CC} = \frac{c_b}{RT}(2c_b\langle\kappa_c(\cosh\bar{\varphi} - 1)\rangle + n_f D_*), \\ &L_{CE} = \frac{Fc_b}{RT}(2\langle\kappa_e(\cosh\bar{\varphi} - 1)\rangle + n_f\Delta_*), \quad L_{EP} = -2Fc_b\langle\kappa_p\sinh\bar{\varphi}\rangle \\ &L_{EC} = \frac{Fc_b}{RT}(-2c_b\langle\kappa_c\sinh\bar{\varphi}\rangle + n_f\Delta_*), \quad L_{EE} = \frac{F^2c_b}{RT}(-2\langle\kappa_e\sinh\bar{\varphi}\rangle + n_f D_*). \end{aligned} \tag{3.38}$$

It should be noted the symmetry of Onsager's matrix $L_{IJ} = L_{JI}$, $(I, J = P, C, E)$ can be verified using the procedure presented by Moyne and Murad (2006) (Section 5.3).

3.3. THE OPEN-CIRCUIT ASSUMPTION

We now proceed by reproducing other related phenomena from our two-scale formulation and establishing the appropriate scenario for introducing new concepts inherent to the problem. Our subsequent development aims at deriving the microscopic representations of the primary/secondary electro-viscous effects (Hunter, 1981; Szymczyk *et al.*, 1999) and of the reflection coefficient discussed in the introduction. We show that these concepts are tied up directly to the absence of an electric current in a confined medium such that no swelling occurs in the transversal direction ($\mathbf{u} = 0$). The one-dimensional version of the electroneutrality condition (2.22) reduces to

$$\frac{dI_e}{dx} = 0, \rightarrow I_e = \text{cte}.$$

In the open-circuit assumption, macroscopic boundary conditions characterizing the absence of an electric current are enforced. This constraint leads to the condition $I_e = \text{cte} = 0$ which reduces the one-dimensional (axial)

form of Onsager's relations (3.37) to the form

$$v_D = -L_{PP}\frac{dp_b}{dx} - L_{PC}\frac{RT}{c_b}\frac{dc_b}{dx} - L_{PE}\frac{d\psi_b}{dx}, \tag{3.39}$$

$$J_c = -L_{CP}\frac{dp_b}{dx} - L_{CC}\frac{RT}{c_b}\frac{dc_b}{dx} - L_{CE}\frac{d\psi_b}{dx},$$

$$0 = -L_{EP}\frac{dp_b}{dx} - L_{EC}\frac{RT}{c_b}\frac{dc_b}{dx} - L_{EE}\frac{d\psi_b}{dx}. \tag{3.40}$$

Hence, eliminating $d\psi_b/dx$ from (3.40), substituting in the relations for v_D and J_c and making use of the symmetry of L_{IJ} we obtain

$$v_D = -L^*_{PP}\frac{dp_b}{dx} - L^*_{PC}\frac{RT}{c_b}\frac{dc_b}{dx}, \tag{3.41}$$

$$J_c = -L^*_{PC}\frac{dp_b}{dx} - L^*_{CC}\frac{RT}{c_b}\frac{dc_b}{dx}, \tag{3.42}$$

where the new coefficients are given by

$$L^*_{PP} = \left(L_{PP} - \frac{L^2_{EP}}{L_{EE}}\right), \qquad L^*_{PC} = \left(L_{PC} - \frac{L_{EP}L_{EC}}{L_{EE}}\right), \tag{3.43}$$

$$L^*_{CP} = \left(L_{CP} - \frac{L_{CE}L_{EP}}{L_{EE}}\right), \quad L^*_{CC} = \left(L_{CC} - \frac{L^2_{CE}}{L_{EE}}\right)$$

and the symmetry property $L_{IJ} = L_{JI}$ has been used. The microscopic representations for $L^*_{IJ}(I, J = C, P)$ can easily be derived by combining the above result with (3.38). Equations (3.42) are consistent with the results of Gu *et al.*, 1998 and show that under the open-circuit assumption Darcy's law and the overall flux of the ions can be represented in terms of pressure and concentration gradients.

An essential feature inherent to the above result is the phenomenon of anomalous (reverse) osmosis. In contrast to the osmotic effect where solvent moves toward the regions of high concentration, in the anomalous case fluid flows in the opposite direction (Gu *et al.*, 1998). Such phenomenon occurs whenever $L^*_{PC} > 0 \rightarrow L_{PC}L_{EE} > L_{EP}L_{EC}$. This corresponds to the case wherein the chemico-osmotic dominates the electro-osmotic component under a constant bulk phase pressure.

Furthermore, if we solve for the pressure gradient in (3.40) and combine with Darcy's law (3.39) we obtain

$$v_D = -L^{**}_{PC}\frac{RT}{c_b}\frac{dc_b}{dx} - L^{**}_{PE}\frac{d\psi_b}{dx} \tag{3.44}$$

with

$$L^{**}_{PC} = \left(L_{PC} - \frac{L_{PP}L_{EC}}{L_{EP}}\right), \qquad L^{**}_{PE} = \left(L_{PE} - \frac{L_{PP}L_{EE}}{L_{EP}}\right).$$

On the right-hand side of (3.41) and (3.44) represents the gradient of the *membrane potential* which measures the total driving force for fluid flow in the absence of electric current (see Gu *et al.*, 1998). These equations consist of two alternative ways of representing this overall driving force in terms of the gradient of the primary unknowns.

3.3.1. *Primary/Secondary Electro-Viscous Effect*

The open-circuit constraint can be further explored to introduce the so-called electroviscous effect EV. Classically EV is envisaged as an increase in the apparent viscosity of the electrolyte solution (compared with its bulk counterpart value μ_f) owing to the counter electro-osmotic flow induced by the streaming potential gradient. This fluid movement opposing the pressure gradient driven flow develops to fulfill the condition of zero electric current (Yang and Li, 1998). As the viscosity is lumped in the hydraulic conductivity, we define the electroviscous effect by the ratio L^*_{PP}/L_{PP}. Such definition aims at quantifying the relative decrease in the hydraulic conductivity due to the back electro-osmotic flow. We then have from (3.43) and (3.38)

$$EV = \frac{L^*_{PP}}{L_{PP}} = 1 - \frac{L^2_{PE}}{L_{PP}L_{EE}} = 1 - \frac{K_E^2}{RTK_P c_b(n_f D_* - 2\langle \kappa_e \sinh \bar{\varphi}\rangle)}. \tag{3.45}$$

The above result furnishes a precise microscopic representation for $EV (0 < EV < 1)$ which will be further exploited numerically. Likewise the electro-osmotic and chemico-osmotic permeabilities, EV incorporates the contribution of the primary effect mainly dictated by the magnitude of the ζ-potential and the secondary component due to the overlapping between the e.d.l.s (Szymczyk *et al.*, 1999; Hunter, 1981).

In the asymptotic thin e.d.l. regime $\bar{\varphi}$ decays sharply from $\bar{\zeta}$ at the particle surface to zero within a thin boundary layer. Together with (3.21) this leads to the approximation

$$\begin{aligned}\langle \exp(\bar{\varphi})\rangle^f \approx \langle \exp(-\bar{\varphi})\rangle^f \approx 1, \text{ and } 2\langle \kappa_e \sinh \bar{\varphi}\rangle) \\ \approx -\frac{2n_f \tilde{\varepsilon}\tilde{\varepsilon}_0 \zeta RT}{F\mu_f}\langle \sinh \bar{\varphi}\rangle \approx 0 \quad \text{for } \ell_D \ll H.\end{aligned}$$

Using the above approximation in (3.36) gives

$$n_f D_* \approx n_f(\mathcal{D}_+ + \mathcal{D}_-) \quad \text{for } \ell_D \ll H$$

in which when combined with (3.45) along with (3.21) yields

$$EV = 1 - \frac{K_E^2}{RT K_P c_b n_f (\mathcal{D}_+ + \mathcal{D}_-)}$$
$$= 1 - \frac{n_f \tilde{\varepsilon}^2 \tilde{\varepsilon}_0^2 \zeta^2 RT}{F^2 \mu_f^2 K_P c_b (\mathcal{D}_+ + \mathcal{D}_-)} \text{ for } \ell_D \ll H.$$

3.4. REFLECTION COEFFICIENT

The well-known concept of reflection coefficient ω has been historically introduced to quantify the nonideal behavior of semi-permeable membranes. According to the classical definition, an ideal membrane totally impervious to the passage of solutes owing to their larger size and open to the movement of the solvent is characterized by $\omega = 1$. The partial mobility of solutes in a nonideal semi-permeable medium is quantified by a $\omega < 1$. Here, unlike the nonionic case ruled by size effects, charged solutes are treated as point charges and the constraints imposed on their movement arise from the chemico and electro-osmotic interactions with the clay particles. Therefore, a comprehensive definition for the reflection coefficient for point charged species requires the correct understanding of the physics underlying such concept, totally different of the nonionic case. To introduce ω we begin by considering the movement of the water as a solvent with a given molar concentration c_{bw} and driven by its bulk chemical potential μ_{bw}. Following Callen (1985), for ideal solutions we adopt instead the representation for the chemical potential in terms of the molar fraction of the bulk water $x_w \equiv c_{bw}/(c_{bw} + 2c_b)$ (recall that $2c_b = c_{b+} + c_{b-}$ in the apparent bulk fluid). We then have

$$\mu_{bw} \equiv \bar{\mu}_{bw} + \frac{1}{c_{bw}}(p_b - p^{\ominus}) + RT \ln x_w, \tag{3.46}$$

where $\bar{\mu}_{bw}$, is the chemical potential of pure water at temperature T and reference pressure $p^{\ominus}$. In the dilute solution approximation, the solvent concentration is equal to that of pure water $c_{bw} = \bar{c}_{bw}$, assumed constant. In addition, since solute concentrations are assumed small in dilute solutions, the term involving $\ln x_w$ in the above expression can be linearized around $c_b = 0$ yielding

$$\ln x_w = \ln\left(1 - \frac{2c_b}{c_{bw} + 2c_b}\right) \approx -\frac{2c_b}{c_{bw}} + \mathcal{O}(c_b)^2 \approx -\frac{2c_b}{\bar{c}_{bw}} + \mathcal{O}(c_b)^2.$$

Thus, using the above approximation in (3.46) gives

$$\mu_{bw} = \bar{\mu}_{bw} + \frac{1}{\bar{c}_{bw}}(p_b - p^{\ominus} - 2RTc_b). \tag{3.47}$$

To introduce the reflection coefficient we define the permeabilities

$$K_{\mathrm{P}}^{*} \equiv L_{\mathrm{PP}}^{*} \quad \text{and} \quad K_{\mathrm{C}}^{*} \equiv \frac{RTL_{\mathrm{PC}}^{*}}{c_{\mathrm{b}}} \tag{3.48}$$

and rephrase the one-dimensional form of Darcy's law (3.41) in the form

$$v_{\mathrm{D}} = -K_{\mathrm{P}}^{*}\frac{\mathrm{d}p_{\mathrm{b}}}{\mathrm{d}x} - K_{C}^{*}\frac{\mathrm{d}c_{\mathrm{b}}}{\mathrm{d}x}. \tag{3.49}$$

In the case of a perfect solute barrier, Darcy's seepage velocity coincides with the velocity of the solvent driven by $\mathrm{d}\mu_{\mathrm{b}w}/\mathrm{d}x$. This ideal situation can be reproduced by setting $K_{\mathrm{C}}^{*} = -2RTK_{\mathrm{P}}^{*}$ in (3.49) and using (3.47) to obtain

$$v_{\mathrm{D}} = -K_{\mathrm{P}}^{*}\left(\frac{\mathrm{d}p_{\mathrm{b}}}{\mathrm{d}x} - 2RT\frac{\mathrm{d}c_{\mathrm{b}}}{\mathrm{d}x}\right) = -\bar{c}_{\mathrm{b}w}K_{\mathrm{P}}^{*}\frac{\mathrm{d}\mu_{\mathrm{b}w}}{\mathrm{d}x} \quad \text{(for a perfect membrane).} \tag{3.50}$$

The comparison between (3.50) and (3.49) together with (3.48) and (3.43) suggest the following definition for the reflection coefficient

$$\omega = -\frac{1}{2RT}\frac{K_{\mathrm{C}}^{*}}{K_{\mathrm{P}}^{*}} = -\frac{1}{2c_{\mathrm{b}}}\frac{L_{\mathrm{PC}}^{*}}{L_{\mathrm{PP}}^{*}} = -\frac{1}{2c_{\mathrm{b}}}\left(\frac{L_{\mathrm{PC}}L_{\mathrm{EE}} - L_{\mathrm{EP}}L_{\mathrm{EC}}}{L_{\mathrm{PP}}L_{\mathrm{EE}} - L_{\mathrm{EP}}^{2}}\right),$$

where on the right-hand side can be computed from the microscopic representations (3.38). Thus, using the above definition in (3.49), Darcy's law can be rewritten in terms of ω in the form

$$v_{\mathrm{D}} = -K_{\mathrm{P}}^{*}\left(\frac{\mathrm{d}p_{\mathrm{b}}}{\mathrm{d}x} - 2\omega RT\frac{\mathrm{d}c_{\mathrm{b}}}{\mathrm{d}x}\right),$$

which is consistent with the classical way of envisaging the role of the reflection coefficient in Darcy's law. Our two-scale formulation is capable of providing as microscopic representation for ω under the open-circuit assumption.

4. Computational Results

We now consider the numerical solution of the closure problems and the development of the constitutive dependence of the effective coefficients on salinity and particle distance. Since the magnitude of the effective parameters is tied-up directly to the local e.d.l. potential, we then begin by discretizing the Poisson–Boltzmann problem.

4.1. NUMERICAL SOLUTION OF POISSON–BOLTZMANN

In order to derive the numerical solution of the one-dimensional Poisson–Boltzmann problem (2.5) (a), we rephrase this equation in terms of the dimensionless transversal coordinate $\bar{y} = y/\ell_D$. This yields

$$\frac{\mathrm{d}^2\bar{\varphi}}{\mathrm{d}\bar{y}^2} = \sinh(\bar{\varphi}), \tag{4.1}$$

$$\frac{\mathrm{d}\bar{\varphi}}{\mathrm{d}\bar{y}} = 0 \quad \text{at } \bar{y} = 0, \tag{4.2}$$

$$\frac{\mathrm{d}\bar{\varphi}}{\mathrm{d}\bar{y}} = \frac{\sigma}{\sqrt{2\tilde{\varepsilon}\tilde{\varepsilon}_0 RTc_\mathrm{b}}} \quad \text{at } \bar{y} = \frac{H}{\ell_\mathrm{D}}. \tag{4.3}$$

By rewriting (3.16) in terms of $\bar{y}$ we obtain

$$\frac{\mathrm{d}\bar{\varphi}}{\mathrm{d}\bar{y}} = -\sqrt{2(\cosh\bar{\varphi} - \cosh\bar{\varphi}_0)} \quad \text{or} \quad \mathrm{d}\bar{y} = -\frac{\mathrm{d}\bar{\varphi}}{\sqrt{2(\cosh\bar{\varphi} - \cosh\bar{\varphi}_0)}}. \tag{4.4}$$

To solve (4.4) we adopt the following changes of variables (see Derjaguin *et al.*, 1987)

$$\sin\alpha = \frac{1}{\cosh(\bar{\varphi}_0/2)} \text{ with } \cot\alpha = \sinh(\bar{\varphi}_0/2) \quad 0 \leqslant \alpha \leqslant \frac{\pi}{2},$$
$$\cos\theta = \frac{\sinh(\bar{\varphi}_0/2)}{\sinh(\bar{\varphi}/2)} \quad 0 \leqslant \theta \leqslant \frac{\pi}{2}. \tag{4.5}$$

Making use of the identity

$$\cosh\bar{\varphi} = 2\cosh^2(\bar{\varphi}/2) - 1 = 2\sinh^2(\bar{\varphi}/2) + 1 \tag{4.6}$$

we obtain

$$\begin{aligned} 2(\cosh\bar{\varphi} - \cosh\bar{\varphi}_0) &= 4\left(\sinh^2(\bar{\varphi}/2) - \sinh^2(\bar{\varphi}_0/2)\right) \\ &= 4\sinh^2\left(\frac{\bar{\varphi}_0}{2}\right)\left(\frac{1}{\cos^2\theta} - 1\right) \\ &= 4\sinh^2\left(\frac{\bar{\varphi}_0}{2}\right)\frac{\sin^2\theta}{\cos^2\theta} = 4\frac{\cos^2\alpha\sin^2\theta}{\sin^2\alpha\cos^2\theta}. \end{aligned} \tag{4.7}$$

By differentiating (4.5)(c), we also have

$$d\left(\sinh\left(\frac{\bar{\varphi}}{2}\right)\right) = \frac{1}{2}\cosh\left(\frac{\bar{\varphi}}{2}\right)\mathrm{d}\bar{\varphi} = \mathrm{d}\left(\frac{\sinh(\bar{\varphi}_0/2)}{\cos\theta}\right) = \sinh\left(\frac{\bar{\varphi}_0}{2}\right)\frac{\sin\theta\,\mathrm{d}\theta}{\cos^2\theta}.$$

Combining the above result with (4.5) we obtain

$$\cosh(\bar{\varphi}/2) = \sqrt{1 + \sinh^2(\bar{\varphi}/2)} = \sqrt{1 + \frac{\sinh^2(\bar{\varphi}_0/2)}{\cos^2\theta}} = \sqrt{1 + \frac{\cos^2\alpha}{\sin^2\alpha\cos^2\theta}}. \tag{4.8}$$

Using (4.5)(b), and (4.7) and (4.8) in (4.4)(b) we obtain

$$\begin{aligned} \mathrm{d}\bar{y} &= -\frac{\mathrm{d}\bar{\varphi}}{\sqrt{2(\cosh\bar{\varphi}-\cosh\bar{\varphi}_0)}} = \frac{2\sinh(\bar{\varphi}_0/2)\sin\theta\,\mathrm{d}\theta}{\sqrt{2(\cosh\bar{\varphi}-\cosh\bar{\varphi}_0)}(\cosh(\bar{\varphi}/2)\cos^2\theta} \\ &= 2\sinh(\bar{\varphi}_0/2)\frac{\sin\theta\,d\theta}{\cos^2\theta\sqrt{1+\frac{\cos^2\alpha}{\sin^2\alpha\cos^2\theta}}}\frac{\cos\theta}{2\sinh(\bar{\varphi}_0/2)\sin\theta} \\ &= \frac{\mathrm{d}\theta}{\sqrt{\cos^2\theta+\frac{\cos^2\alpha}{\sin^2\alpha}}} = \frac{\mathrm{d}\theta}{\sqrt{1-\sin^2\theta+\frac{1}{\sin^2\alpha}-1}}, \end{aligned}$$

which implies

$$\mathrm{d}\bar{y} = \frac{\sin\alpha\,\mathrm{d}\theta}{\sqrt{1-\sin^2\alpha\,\sin^2\theta}}.$$

Integrating the above result and noting from (4.5)(c) that $\theta = 0$ at $\bar{y} = 0$ yields

$$\bar{y} = \int_0^{\theta} \frac{\sin\alpha\,\mathrm{d}\theta}{\sqrt{1-\sin^2\alpha\,\sin^2\theta}}. \tag{4.9}$$

We now turn to the task of rephrasing boundary condition (4.3). From (4.4)(a) to (4.7) we have

$$\frac{\mathrm{d}\bar{\varphi}}{\mathrm{d}\bar{y}} = -\sqrt{2(\cosh\bar{\varphi}-\cosh\bar{\varphi}_0)} = -2\frac{\cos\alpha\sin\theta}{\sin\alpha\cos\theta}$$

in which when combined with (4.3) gives

$$\frac{-\sigma}{\sqrt{2\tilde{\epsilon}\tilde{\epsilon}_0 RTc_{\mathrm{b}}}} = 2\frac{\cos\alpha\sin\theta_1}{\sin\alpha\cos\theta_1} \quad \text{at } \bar{y} = H/L_{\mathrm{D}}, \tag{4.10}$$

where $\theta = \theta_1$, when $\bar{y} = H/\ell_{\mathrm{D}}$. The problem given by (4.9) and boundary condition (4.10), formulated in terms of the unknowns α and θ_1 can be rewritten as

$$\frac{H}{\ell_{\mathrm{D}}} = \int_0^{\theta_1} \frac{\sin\alpha\,\mathrm{d}\theta}{\sqrt{1-\sin^2\alpha\,\sin^2\theta}} \tag{4.11}$$

$$\tan\theta_1 = \frac{-\sigma}{2Fc_{\mathrm{b}}\ell_{\mathrm{D}}}\tan\alpha. \tag{4.12}$$

For each pair $\{c_{\mathrm{b}}, H\}$, we compute the Debye's length through its definition. Given ℓ_{D} and H, Equations (4.11) and (4.12) define a nonlinear system in terms of $\{\alpha, \theta_1\}$ which can easily be solved within any iterative integration scheme. After computing α we make use of (4.5)(a) and compute $\bar{\varphi}_0$. Then we proceed by incrementing (4.9) from $\bar{y} = 0$ to H/ℓ_{D} and

also using (4.5) (c) compute the local distributions $\theta = \theta(\bar{y})$ and $\bar{\varphi} = \bar{\varphi}(\bar{y})$ parametrized by $\{c_b, H\}$. Further, using the numerical distribution of the e.d.l. potential in (3.19) and (3.22) furnishes the discrete electroosmotic and chemico-osmotic characteristic velocity profiles $\{\kappa_c, \kappa_e\}$. Finally by averaging the local distributions in the transversal direction yields the constitutive dependence of the effective electro-chemical parameters on $\{c_b, H\}$. In particular the above change of variables furnish a straightforward relation for the disjoining/swelling pressure (recall that $\Pi_d = \Pi_S$ for parallel particles) in terms of $\{c_b, \alpha\}$. In fact using (4.6) in (3.32) gives

$$\Pi_d = 2c_b RT(\cosh \bar{\varphi}_0 - 1) = 4c_b RT \sinh^2\left(\frac{\bar{\varphi}_0}{2}\right)$$

in which when combined with (4.5) (b) gives

$$\Pi_d = \frac{4RTc_b}{\tan^2 \alpha}.$$

4.2. NUMERICAL SIMULATIONS

In what follows we present the numerical behavior of the local e.d.l. potential and velocity profiles along with the constitutive behavior of the effective coefficients. In the simulations we adopt $\sigma = -0.2\,\mathrm{cm}^{-2}$. Denoting $y^* = y/H$ and $\bar{E} \equiv FEH/RT$ a dimensionless electric field, the plots $\bar{\varphi} = \bar{\varphi}(y^*)$ and $\bar{E} = \bar{E}(y^*)$ are depicted in Figure 2 for two values of c_b and H/ℓ_D. The ticks in the left and right margins show the range of values of $\bar{\varphi}$ and $\bar{E}$, respectively. As expected, in the line of symmetry ($y = 0$), $\bar{\varphi}$ attains its maximum value and decreases negatively in a symmetric fashion toward the location of the particles $y^* = \pm 1$. Owing to symmetry, the electric field vanishes at $y^* = 0$ and behaves in a skew symmetric fashion with y^*.

In Figure 3 we depict the local behavior of the normalized (unitary averaged) characteristic velocity profiles $\kappa_i^* = \kappa_i / K_I$ (i = p, c, e and $I = P, C, E$) for two values of H/ℓ_D and c_b. The hydraulic characteristic function κ_p^* is nothing but the classical parabolic profile whereas κ_c^* and κ_e^* are strongly influenced by the interaction with the e.d.l.'s. For small electrokinetic distances ($H/\ell_D = 1$), when the overlapping between the e.d.l.'s is pronounced, the chemical osmosis and electro-osmosis velocity profiles resemble each other but somewhat differ from the parabolic (Figure 3(a)). For large distances ($H/\ell_D = 10$) both chemico-osmotic and Smoluchowski electroosmotic profile dictated by the $\bar{\zeta}$-potential at the surface, exhibit steeper gradient near the walls and a flat profile in the center of the micro-pore. In this regime both profiles can simply be modeled by a 'slip' in the velocity near the wall as depicted in Figure 3(b).

Figures 4–6 display the macroscopic conductivities $\{K_P, K_C, K_E\}$ in Darcy's law obtained by averaging the corresponding velocity profiles

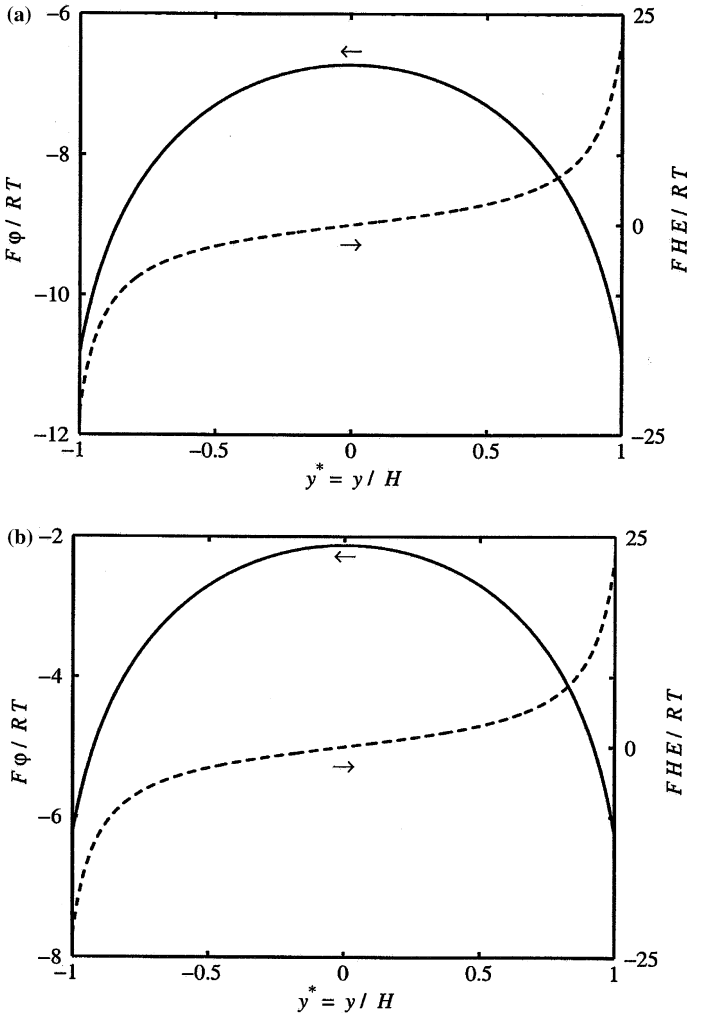

Figure 2. Local electric potential and electric field distributions: (a) $H/L_D = 0.1$ and $c_b = 2.32 \times 10^{-4}$ mol/l; (b) $H/L_D = 1.0$ and $c_b = 2.32 \times 10^{-2}$ mol/l.

$\{\kappa_p, \kappa_c, \kappa_e\}$. As expected, the magnitude of K_P is solely dictated by particle distance H. On the other hand K_C and K_E decrease with the salinity owing to the interaction of the local velocity profiles with the e.d.l.s. The asymptotic range $H \to \infty$ of thin e.d.l.s corresponds to the highest values of K_E and K_C, solely dictated by the ζ-potential according to (3.21) and (3.30).

Figure 7 shows the behavior of the averaged diffusion coefficient $D_\pm = D_\pm^c = D_\pm^e = \langle \mathcal{D}_\pm \exp(\pm\bar{\varphi}) \rangle^f$ (recall that $D_\pm^p = 0$ in the stratified arrangement). Since $\bar{\varphi} < 0$, the effect of the e.d.l. is to magnify and reduce the diffusivities of the counter-ions and co-ions, respectively. The disparity between D_+

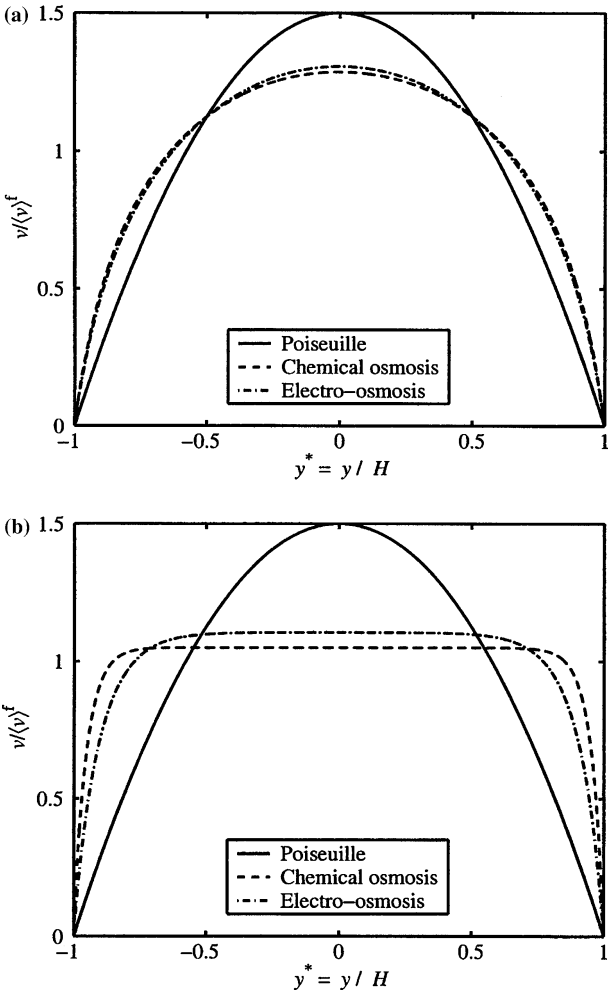

Figure 3. Normalized velocity profiles: (a) $H/\ell_D = 1$ and $c_b = 2.32 \times 10^{-2}$ mol/l; (b) $H/\ell_D = 10$ and $c_b = 2.32$ mol/l.

and D_- increases as the e.d.l. effects are amplified with the decrease in c_b and H.

Figure 8 shows the disjoining pressure plots typical of a Gouy–Chapman scenario (Hunter, 1994; Van Olphen, 1977; Lyklema, 1993). As is easily seen the magnitude of Π_d reduces with the increase in c_b and H. In addition, from (3.35) one may note that the same plot scaled by n_s/c_s also describes the constitutive behavior of the electro-chemical compressibility γ_π. A similar behavior is also verified for the surface tension of the electrolyte solution σ_{fs} as depicted in Figure 9, though one may observe that for high salinities ($c_b \approx 1$ mol/l), σ_{fs} does not vary with H.

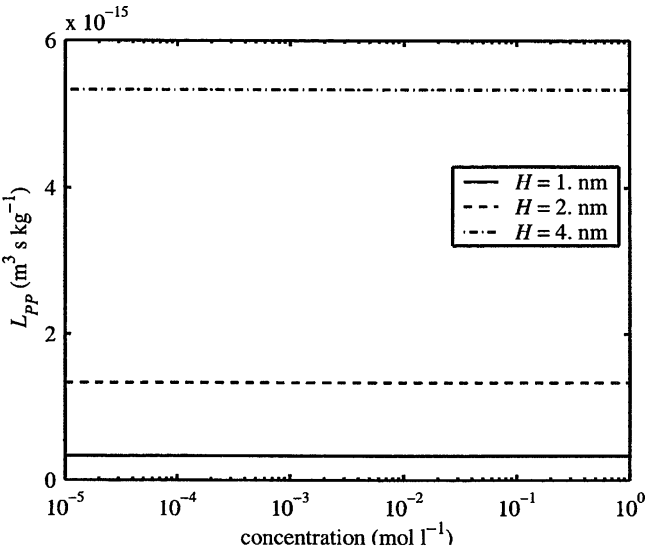

Figure 4. Behavior of the hydraulic conductivity K_P (or the Onsager's coefficient L_{PP}) with c_b for $H = 1, 2$ and 4 nm.

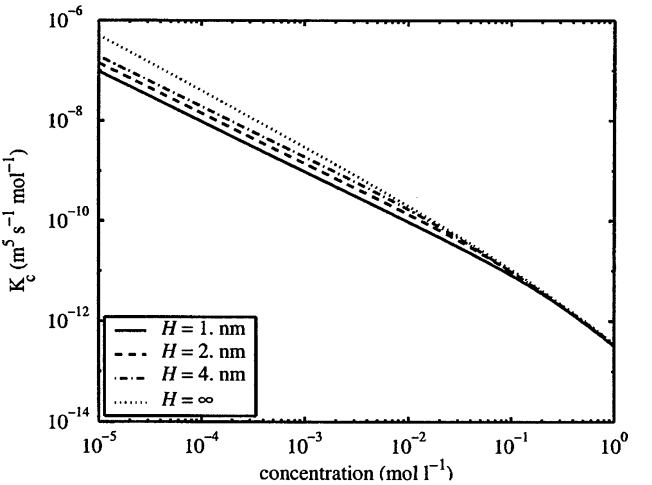

Figure 5. Behavior of the chemico-osmotic permeability K_C with c_b for $H = 1, 2, 4$ nm and ∞

Figures 10–13 display the behavior of the Onsager's coefficients $\{L_{PC}, L_{CE}, L_{CC}, L_{EE}\}$ as a function of c_b and H. By invoking the symmetry, from (3.38) the plots of K_P and K_E also describe L_{PP} and $L_{PE} = L_{EP}$, respectively. The behavior of the off-diagonal coefficients $\{L_{PC}, L_{CE}\}$ resemble each other, showing a similar decrease with c_b and H as depicted in Figures 10 and 11. Nevertheless the electro-migration component L_{CE}

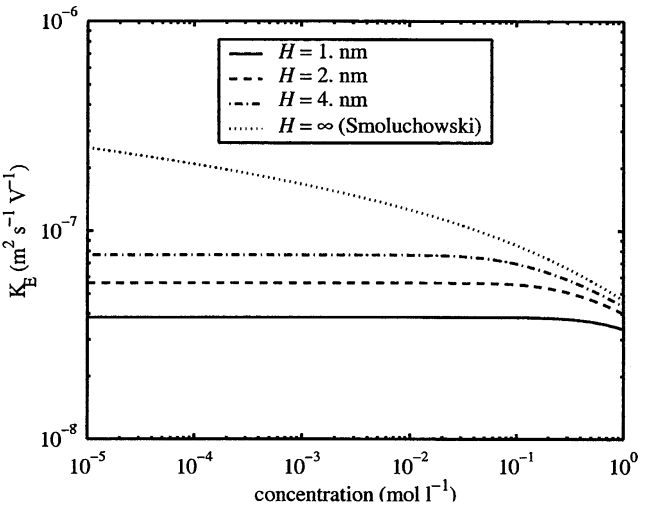

Figure 6. Behavior of the electro-osmotic permeability K_E (or the Onsager's coefficient L_{PE}) with c_b for $H = 1, 2$ and 4 nm.

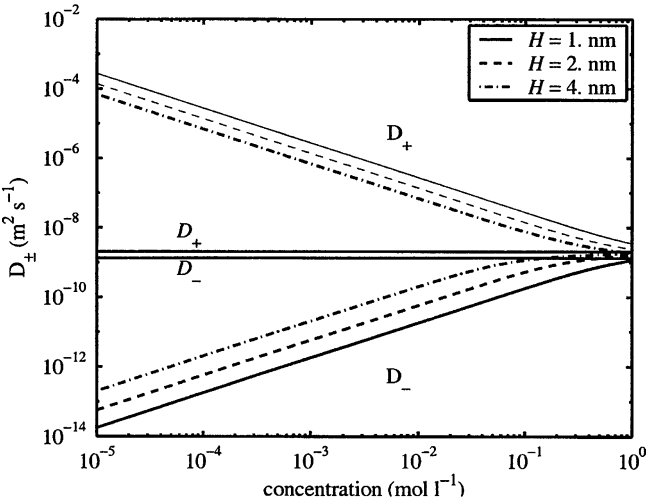

Figure 7. Behavior of the diffusivities $D_{\pm} = D^c_{\pm} = D^e_{\pm}$ with c_b for $H = 1, 2$ and 4 nm.

exhibits a steeper gradient for high c_b. The diagonal Onsager's coefficients are displayed in Figures 12 and 13. By invoking the microscopic representation of $\{L_{CC}, L_{EE}\}$ in (3.38) one may note that for high c_b, where the contribution from the e.d.l. potential becomes weaker, the magnitude of the Onsager's parameters is mainly dictated by the term involving the sum of cation and anion diffusivities D_*. Recalling the numerical behavior of the diffusivities in Figure 7, as c_b increases, the magnitude of $\{L_{CC}, L_{EE}\}$ becomes dominated by the grow of D_-. This leads to an asymptotic

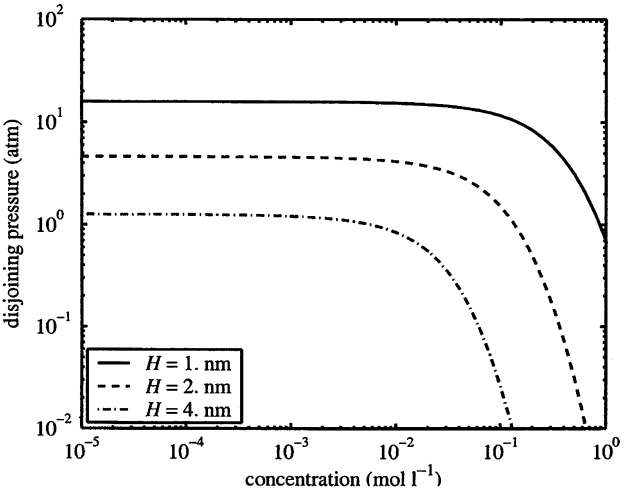

Figure 8. Behavior of the disjoining pressure Π_d with c_b for $H = 1, 2$ and 4 nm.

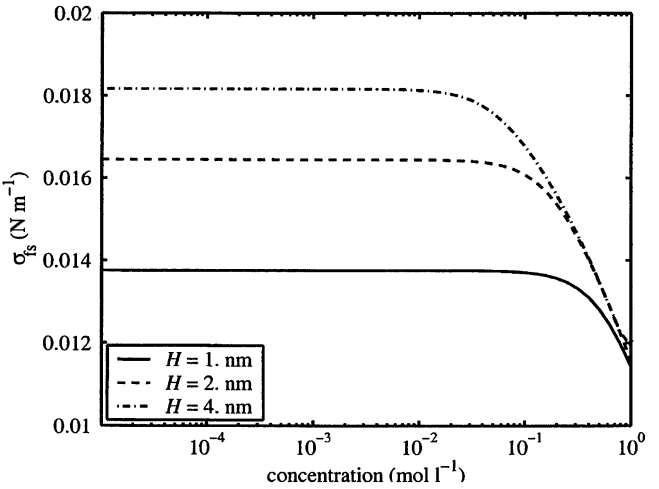

Figure 9. Behavior of the surface tension σ_{fs} with c_b for $H = 1, 2$ and 4 nm.

behavior of diffusivity grow with concentration, typical of nonionic species, as one may observe in Figures 12 and 13.

In Figure 14 we display the numerical behavior of the electroviscous effect EV. For large particle distances ($H > 4$ nm) EV becomes dictated by the primary effect, solely given by the magnitude of the $\bar{\zeta}$-potential. As H decreases, the secondary effect due to the overlapping of the e.d.l.s becomes more pronounced leading to a magnification of EV, as one may verify in the other curves. In addition, one may also observe that for H fixed, EV remains constant for a considerable range ($c_b < 5 \times$

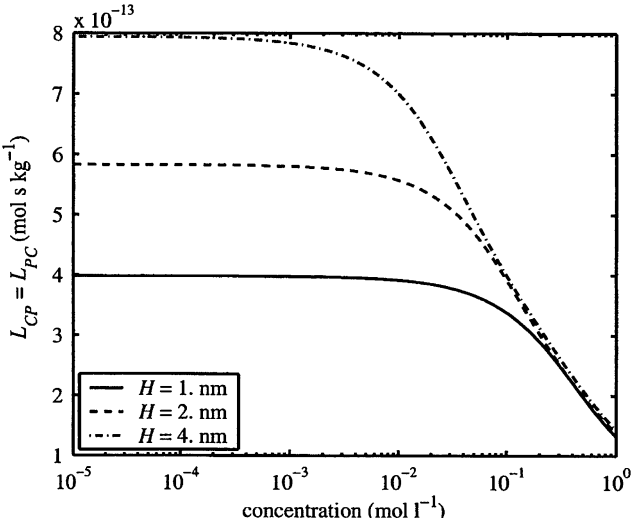

Figure 10. Behavior of the Onsager's coefficient L_{PC} with c_{b} for $H = 1, 2$ and 4 nm.

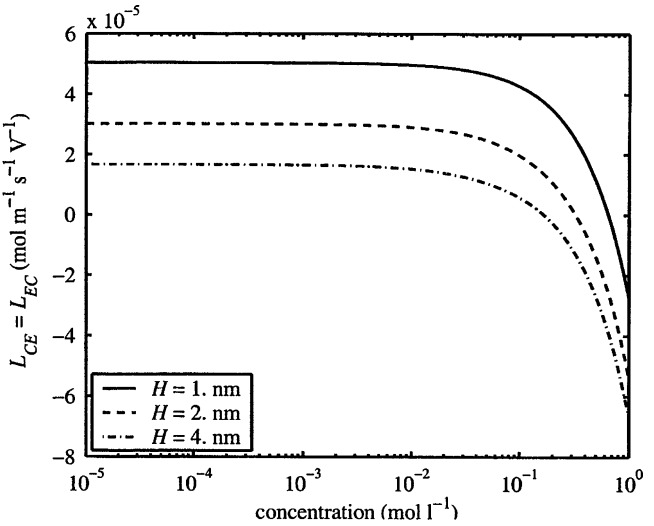

Figure 11. Behavior of the Onsager's coefficient L_{CE} with c_{b} for $H = 1, 2$ and 4 nm.

10^{-2} mol/l). Conversely, in the other range EV exhibits high decrease with salinity. Finally, Figure 15 shows the numerical behavior of the reflection coefficient ω. For low $c_{\mathrm{b}} (< 10^{-3}$mol/l), where e.d.l. effects are relevant, the strong binding of the ions restrict their movement and therefore the clay behaves as a quasi-perfect membrane with $\omega \approx 1$ independent of c_{b}. As e.d.l. effects become weaker with the grow in c_{b} the magnitude of ω decreases. For high salt concentration ($c_{\mathrm{b}} > 5 \times 10^{-1}$mol/l) and $H > 2$ nm

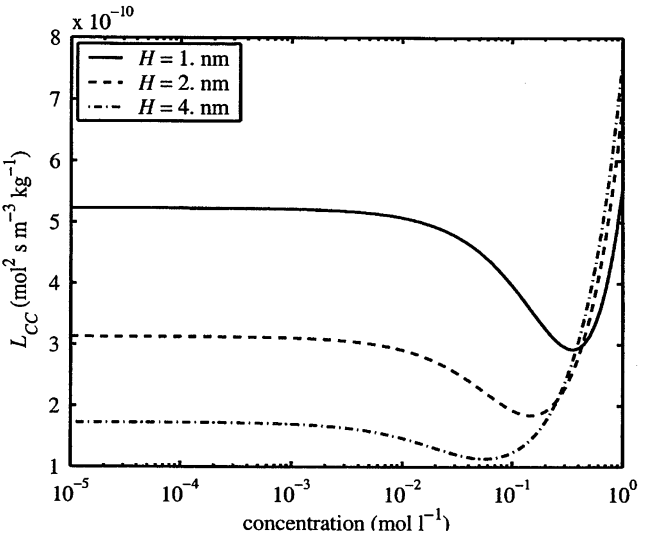

Figure 12. Behavior of the Onsager's coefficient L_{CC} with c_b for $H = 1, 2$ and 4 nm.

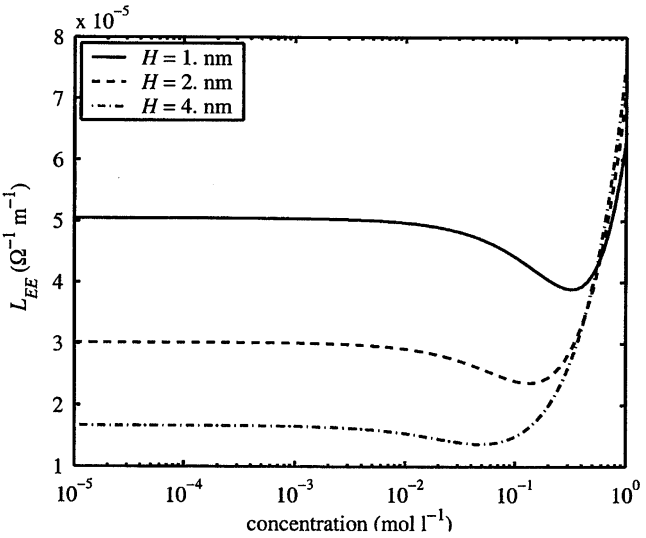

Figure 13. Behavior of the Onsager's coefficient L_{EE} with c_b for $H = 1, 2$ and 4 nm.

one may observe negative values of the reflection coefficient corresponding to the reverse osmosis phenomenon associated with flow from high to low concentrations. The numerical behavior obtained herein resembles in form the experimental result reported in Barbour and Fredlund (1989).

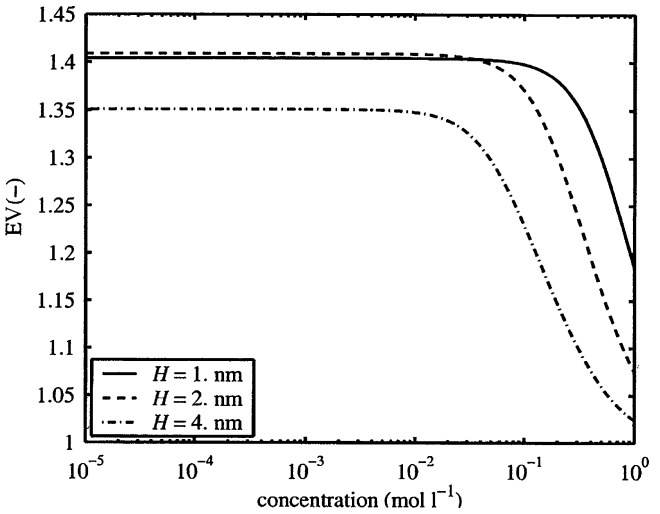

Figure 14. Behavior of the electro-viscous effect EV with c_b for $H = 1, 2$ and 4 nm.

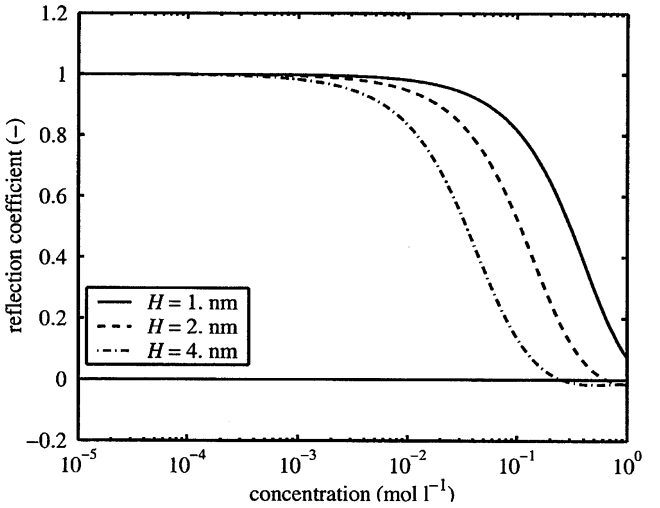

Figure 15. Behavior of the reflection coefficient ω with c_b for $H = 1, 2$ and 4 nm

5. Conclusion

In this article we validated computationally the two-scale model for swelling compacted clays proposed in Moyne and Murad (2006) and established the proper scenario for introducing the new concepts of interfacial tension of the electrolyte solution, primary/secondary electroviscous effects and reflection coefficient. By considering the clay microstructure composed

of parallel particles of face-to-face contact the local closure problems were numerically solved and the constitutive behavior of the effective electro-chemo-mechanical coefficients derived in Moyne and Murad (2006) and the new quantities introduced herein were computed for different values of salinity and particle separation.

The computational results obtained herein show a strong dependence of the effective electrochemo-mechanical coefficient on the local Poisson–Boltzmann distribution of the microscale e.d.l. potential. Such correlation provides a first attempt at bridging the gap between the numerical constitutive behavior of the effective electro-chemo-mechanical coefficients and the microstructural behavior of swelling colloids.

Further work is required to incorporate tortuosity effects by solving the general form of the closure problem in nonparallel particle arrangements. In this more complex microscopic portrait of the swelling medium, additional effects must be incorporated in the macroscopic model through the local gradients of the purely mechanical characteristic functions $\{\boldsymbol{\zeta}\boldsymbol{\xi}\}$ and of the electro-chemical functions $\{\boldsymbol{f}^{\pm}, h_I^{\pm}\}(I = \mathrm{p}, \mathrm{c}, \mathrm{e})$ which capture the dynamical interaction with the fluctuation of the electrical double layers. This will be further investigated.

Finally we remark that though the tangential interfacial tension of the liquid has no effect in disjoining the solid matrix in the parallel particle arrangement, this quantity may play an important role in swelling when considering random cell geometries. The relative roles of the swelling pressure and interfacial tension in disordered microstructures will also be subject of future work.

Acknowledgements

C.M. and M.M. were supported by the $\mathrm{CNP_q}$-CNRS international cooperation agreement.

References

Auriault, J. L.: 1991, Heterogeneous media: Is an equivalent homogeneous description always possible?, *Int. J. Engng. Sci.* **29**, 785–795.

Auriault, J. L.: 1990, Behavior of porous saturated deformable media, Geomaterials: In: F. Darve (ed.), *Constitutive Equations and Modeling*, Elsevier, New York, pp. 311–328.

Auriault, J. L. and Adler, P. M.: 1995, Taylor dispersion in porous media: Analysis by multiple scale expansions, *Adv. Water Resour.* **18**(4), 217–226.

Auriault, J. L. and et Sanchez-Palencia, E.: 1977, Etude du comportment macroscopique d'un milieu poreux saturé déformable, *J. Mécanique* **16**(4), 575–603.

Babak, V.: 1998, Thermodynamics of plane-parallel liquid films, *Colloids Surfaces A: Physicochem. Engng. Aspects* **142**, 135–153.

Barbour, S. L. and Fredlund, D. G.: 1989, Mechanisms of osmotic flow and volume changes in clay soils, *Canadian Geotech. J.* **26**, 551–562.

Bennethum, L. S., Murad, M. A. and Cushman, J. H.: 2000, Macroscale thermodynamics and the chemical potential for swelling porous media, *Transport Porous Media* **39**, 187–225.

Bensoussan, A., Lions, J. L. and Papanicolaou, G.: 1978, *Asymptotic Analysis for Periodic Structures*, North-Holland, Amsterdam.

Biot, M.: 1941, General theory of three-dimensional consolidation, *J. Appl. Phys.* **12**, 155–164.

Biot, M. and Willis, D. G.: 1957, The elastic coefficients of the theory of consolidation, *J. Appl. Mech.* **79**, 594–601.

Callen, H.: 1985, *Thermodynamics and an Introduction to Thermostatics*, Wiley, New York.

Coelho, D., Shapiro, M., Thovert, J. F. and Adler, P. M.: 1996, Electroosmotic phenomena in porous media, *J. Colloid Interface Sci.* **181**, 169–190.

Derjaguin, B. V., Churaev, N. V. and Muller, V. M.: 1987, *Surface Forces*, Plenum Press, New York.

Derjaguin, B. V. and Churaev, N. V.: 1978, On the question of determining the concept of disjoining pressure and its role in the equilibrium and flow of thin films, *J. Colloid Interface Sci.* **66**(3), 389–398.

Derjaguin, B. V., Dukhin, S. S. and Kobotkova, A. A.: 1961, Diffusiophoresis in electrolyte solutions and its role in the mechanism of film formation from rubber latexes by the method of ionic deposition, *Kolloidn Zh.* **23**(3), 53–55.

Eringen, A. C. and Maugin, G. A.: 1989, *Electrodynamics of Continua*, Springer-Verlag.

Gray, W. G. and Hassanizadeh, S. M.: 1989, Averaging theorems and averaged equations for transport of interface properties in multiphase systems, *Int. J. Multiphase Flow* **15**, 81–95.

Gu, W. Y., Lai, W. M. and Mow, V. C.: 1998a, A triphasic analysis of negative osmotic flows through charged hydrated tissues, *J. Biomech.* **30**(1), 71–78.

Gu, W. Y., Lai, W. M. and Mow, V. C.: 1998b, A mixture theory for charged–hydrated soft tissues containing multi-electrolytes: passive transport and swelling behaviors, *J. Biomech. Engng.* **120**, 169–180.

Hassanizadeh, S. M. and Gray, W. G.: 1990, Mechanics and thermodynamics of multiphase flow in porous media including interphase boundaries, *Adv. Water Resour.* **13**, 169–186.

Hueckel, T.: 1992, On effective stress concepts and deformation in clays subjected to environmental loads, *Canad. Geotech. J.* **29**, 1120–1125.

Hunter, R. J.: 1981, *Zeta Potential in Colloid Science: Principles and Applications*, Academic Press, New York.

Hunter, R. J.: 1994, *Introduction to Modern Colloid Science*, Oxford University Press, Oxford.

Huyghe, J. M. and Janssen, J. D.: 1997, Quadriphasic mechanics of swelling incompressible porous media, *Int. J. Engng. Sci.* **25**(8), 793–802.

Kemper, W. D. and Schaik, J. C.: 1966, Osmotic efficiency coefficients across compacted clays, *Proc. Soil Sci. Soc. America* **30**, 529–534.

Lai, W. M., Hou, J. S. and Mow, V. C.: 1991, A triphasic theory for the swelling and deformation behaviors of articular cartilage, *J. Biomech. Engng.* **113**, 245–258.

Landau, L. D. and Lifshitz, E. M.: 1960, *Electrodynamics of Continuous Media*, Pergamon Press, Oxford.

Lydzba, D. and Shao, J. F.: 2000, Study of poroelasticity material coefficients as response of microstructure, *Mech. Cohesive-Frictional Mater.* **5**, 194–171.

Low, P. F.: 1987, Structural component of the swelling pressure of clays, *Langmuir* **3**, 18–25.

Lyklema, J.: 1993, *Fundamentals of Colloid and Interface Science*, Academic Press, London.

Moyne, C. and Murad, M.: 2002, Electro-chemo-mechanical couplings in swelling clays derived from a micro/macro homogenization procedure, *Int. J. Solids Struct.* **39**, 6159–6190.

Moyne, C. and Murad, M.: 2003, Macroscopic behavior of swelling porous media derived from micromechanical analysis, *Transport Porous Media* **50**, 127–151.

Moyne, C. and Murad, M.: 2006, A Two-scale model for coupled electro-chemo-mechanical phenomena and Onsager's reciprocity relations in expansive clays: I Homogenization analysis, *Transport Porous Media* **62**, 333–380.

Murad, M. A. and Cushman, J. C.: 2000, Thermomechanical theories for swelling porous media with microstructure, *Int. J. Engng. Sci.* **38**(5), 517–564.

Van Olphen: 1977, *An Introduction to Clay Colloid Chemistry; For Clay Technologists, Geologists, and Soil Scientists*, Wiley, New York.

Prieve, D. C., Anderson, J. L., Ebel, J. P. and Lowell, M. E.: 1984, Motion of a particle by chemical gradients. Part 2. Electrolytes, *J. Fluid Mech*. **148**, 247–269.

Samson, E. and Marchand, J.: 1999, Numerical solution of the extended Nernst–Planck model, *J. Colloid Interface Sci.* **215**, 1–8.

Sanchez-Palencia, E.: 1980, *Non-Homogeneous Media and Vibration Theory*, Lecture Notes in Phys., Springer, New York.

Shang, J. Q.: 1997, Zeta potential and electroosmotic permeability of clay soils, *Canad. Geotech. J.* **34**, 627–631.

Sridharan, A. and Rao, G. V.: 1973, Mechanisms controlling volume change of saturated clays and the role of the effective stress concept, *Geotechnique* **23**(3), 359–382.

Szymczyk, A., Aoubiza, B., Fievet, P. and Pagetti, J.: 1999, Electrokinetic phenomena in homogeneous cylindrical pores, *J. Colloid Interface Sci.* **216**, 285–296.

Terada, K., Ito, T. and Kikuchi, N.: 1998, Characterization of the mechanical behaviors of solid-fluid mixture by the homogenization method, *Comput. Meth. Appl. Mech. Engng.* **153**, 223–257.

Toshev, B. V. and Ivanov, I. B.: 1975, Thermodynamics of thin liquid fims. I. Basic relations and conditions of equilibrium, *Colloid Polymer Sci.* **253**, 558–565.

Yang, C. and Li, D.: 1998, Analysis of electrokinetic effects on the liquid flow in rectangular microchannels, *Colloids Surfaces A: Physicochem. Engng. Aspects* **143**, 339–353.

Yeung, A. T. and Mitchell, J. K.: 1993, Coupled fluid, electrical and the chemical flows in soil, *Geotechnique* **43**(1), 121–134.